NATIONAL ADVISORY COMMITTEE FOR AERONAUTICS

TECHNICAL NOTE 3715

COMPARISON OF THE EXPERIMENTAL AND THEORETICAL DISTRIBUTIONS OF LIFT ON A SLENDER INCLINED BODY OF REVOLUTION AT M = 2

By Edward W. Perkins and Donald M. Kuehn

Ames Aeronautical Laboratory
Moffett Field, Calif.

Washington
May 1956

NATIONAL ADVISORY COMMITTEE FOR AERONAUTICS

TECHNICAL NOTE 3715

COMPARISON OF THE EXPERIMENTAL AND THEORETICAL DISTRIBUTIONS OF LIFT ON A SLENDER INCLINED BODY OF REVOLUTION AT M = 2[1]

By Edward W. Perkins and Donald M. Kuehn

SUMMARY

Pressure distributions and force characteristics have been determined for a body of revolution consisting of a fineness ratio 5.75, circular-arc, ogival nose tangent to a cylindrical afterbody for an angle-of-attack range of 0° to 35.5°. The free-stream Mach number was 1.98 and the free-stream Reynolds number was approximately 0.5×10^{6}, based on body diameter.

Comparison of the theoretical and experimental pressure distributions shows that for zero lift, either slender-body theory or higher-order theories yield results which are in good agreement with experiment. For the lifting case, good agreement with theory is found only for low angles of attack and for the region in which the body cross-sectional area is increasing in the downstream direction. Because of the effects of cross-flow separation and the effects of compressibility due to the high cross-flow Mach numbers at large angles of attack, the experimental pressure distributions differ from those predicted by potential theory.

Although the flow about the inclined body was, in general, similar to that assumed as the basis for Allen's method of estimating the forces resulting from viscous effects (NACA RM A9I26), the distribution of the forces was significantly different from that assumed. Nevertheless, the lift and pitching-moment characteristics were in fair agreement with the estimated values.

INTRODUCTION

The need for accurate knowledge of the flow about bodies of revolution has become increasingly important for the design of high-speed missiles and airplanes. For these aircraft the body contribution to the aerodynamic

[1]Supersedes NACA RM A53E01, by Edward W. Perkins and Donald M. Kuehn, 1953.

characteristics of the complete vehicle has assumed greater importance than heretofore. Not only is there need for more accurate knowledge of the flow for the customary low angles of attack but, because of maneuverability requirements, the flow characteristics must be known for a much larger angle-of-attack range.

Since the effects of viscosity play a predominant role in determining the flow over inclined bodies even at moderate angles of attack, the results of potential-flow theories are valid only for small angles of attack. An additional limitation on the range of applicability of certain theories results from the assumption of incompressible cross flow. In reference 1, for instance, it is indicated that the method developed should be applicable as long as the Mach number normal to the inclined axis of the body is not large compared with the critical Mach number for a circular cylinder. However, for supersonic speeds, the Mach number normal to the inclined axis may become so large, even at relatively small angles of attack, that the effects of compressibility on the cross flow can no longer be neglected. One of the purposes of the present investigation is, therefore, to indicate the nature of the effects of both viscosity and cross-flow compressibility and to show wherein the pressure distribution for a slender inclined body of revolution in a supersonic air stream differs from that predicted by available theory.

Although there is no simple theoretical method available for predicting either the viscous or the cross-flow compressibility effects on the pressure distributions, an approximate method to account for these effects on the over-all aerodynamic characteristics was proposed in reference 2. It has been shown (ref. 3) that this method provides an improvement over the prediction of potential theory alone for both the lift and the drag rise. However, it was found that the centers of pressure for the bodies considered were aft of the positions predicted by the approximate theory. Because of this discrepancy, the present experimental investigation of the loading of an inclined body has been undertaken to assess the validity of certain of the assumptions made in the approximate method of reference 2. In particular, the purpose of the present investigation is to determine wherein the magnitude and distribution of the cross forces resulting from viscous effects differ from those assumed in the approximate method. Results of similar studies of pressure distributions and force characteristics of a parabolic-arc body of revolution (NACA RM-10) and an ogive-cylinder body are available in references 4 and 5, respectively.

SYMBOLS

A reference area, $\frac{\pi d^2}{4}$

c_{d_c} section drag coefficient of a circular cylinder based on body diameter

c_{d_c}'	experimental local cross-flow drag coefficient based on body diameter
C_L	lift coefficient, $\frac{L}{q_o A}$
C_m	pitching-moment coefficient about the nose of the model, $\frac{M}{q_o A d} = -\frac{1}{d}\int_0^l C_n\, x\, dx$
C_n	local normal-force coefficient per in., $\frac{2r}{A}\int_0^{\pi}\frac{p}{q_o}\cos\theta\, d\theta$
C_N	total normal-force coefficient, $\int_0^l C_n dx$
d	maximum body diameter
L	lift force
l	body length
l_n	length of ogival nose
M	pitching moment
M_o	free-stream Mach number
M_c	cross-flow Mach number, $M_o \sin\alpha$
p	local static pressure on the model surface
p_o	free-stream static pressure
C_p	pressure coefficient, $\frac{p - p_o}{q_o}$
ΔC_p	lifting pressure coefficient, $C_p - C_{p_{\alpha=0}}$
q_o	free-stream dynamic pressure
Re_o	free-stream Reynolds number per inch
Re_c	cross-flow Reynolds number based on body diameter
x,r,θ	model cylindrical coordinates, origin at the apex ($\theta = 0^o$ in the vertical plane of symmetry on the windward side)
α	angle of attack

APPARATUS AND TESTS

Tunnel

This investigation was conducted in the Ames 1- by 3-foot supersonic wind tunnel No. 1. It is a closed-circuit variable-pressure tunnel in which the Reynolds number is changed by varying the total pressure within the approximate limits of one-fifth of an atmosphere to three atmospheres. Adjustment of the flexible steel plates, which form the upper and lower walls of the nozzle, provides a Mach number range of 1.2 to 2.2.

Models

Two ogive-cylinder models were tested with geometrically similar noses, but with different maximum diameters and different fineness-ratio cylindrical afterbodies. Both models had a 33-1/3-caliber tangent ogive nose (fineness ratio 5.75). All pertinent model dimensions and orifice locations are shown in figure 1.

Tests

The pressure-distribution data for both models were obtained for a Mach number of 1.98 and a free-stream Reynolds number of 0.5×10^6 per inch. Model 1, for which pressure-distribution data were obtained on the cylindrical afterbody only, was tested through the angle-of-attack range of 0° to 35.5°. Because the errors due to the irregularities in the air stream were large compared to the measured pressures for low angles of attack, all the data for angles of attack of less than 10° were discarded. Subsequently, model 2, for which pressure-distribution data were obtained for the nose as well as the cylindrical afterbody, was tested in an improved air stream through the angle-of-attack range of 0° to 15°. Since the models were instrumented with longitudinal rows of orifices, circumferential pressure distributions were obtained by rotating the models through the desired range of circumferential angle (θ) in increments of 15°. All pressures were photographically recorded from a multiple-tube manometer system.

REDUCTION OF DATA

The data were initially reduced to the form of an uncorrected pressure coefficient based upon free-stream conditions at the nose of the model. With the assumption of a two-dimensional stream, the data were then corrected for nonuniformities of the free-stream pressure by a simple linear superposition of these pressure nonuniformities and the measured body pressures. All corrected pressure coefficients for models 1 and 2 are shown in tables I and II, respectively.

The corrected pressure coefficients have been integrated around the body at 23 axial stations on model 1 and at 29 axial stations on model 2 for each angle of attack to obtain the section normal-force coefficients. These force coefficients have been corrected for the effects of local stream angle and stream curvature. For model 2, the loading was known over the complete body length; therefore, total force and moment coefficients were obtained from graphical integration of the corrected cross-force distribution.

PRECISION OF MEASUREMENT

The uncertainty of the experimental data has been determined by consideration of the possible errors of the individual quantities (including corrections) used in the calculation of the final data. These individual errors were combined by the root mean square to give the total uncertainty which is shown in the following tabulation for each parameter:

C_p (in plane of symmetry)	±0.004
C_p (other than in plane of symmetry)	±.006
C_n	±.003
C_L	±.008
C_m	±.056
α	±.1°

The values of the possible uncertainty in C_p appear quite large relative to the scatter of the pressure-distribution data (figs. 5 and 7). However, the possible uncertainty consists, for the most part, of errors which would introduce a constant shift in the entire distribution at a given station or errors which would result in a small gradient. Hence, although these possible errors contribute to the total uncertainty, they are not reflected in the scatter of the data.

RESULTS AND DISCUSSION

Vapor-Screen Studies

Before discussing the results of the pressure measurements, it is appropriate to consider the characteristics of the flow around an inclined body of the type used in this investigation. Limited results describing certain characteristics of the flow as determined with the vapor-screen technique have been given in reference 3. A more detailed consideration is presented in the following discussion.

Vapor-screen studies have shown the existence of vortices in the flow field adjacent to the lee side of an inclined body. These studies have shown that for a given body, the configuration and behavior of the vortices, in addition to depending on the free-stream Reynolds number and Mach number, are strong functions of the angle of attack. The behavior of the vortices with regard to angle-of-attack effects may be roughly divided into three regimes based upon observations of the steadiness and disposition of the vortices at the base of the model: the low angle-of-attack regime in which a steady symmetric pair is formed, the intermediate range in which a steady asymmetric configuration of two vortices exists, and the high angle range in which an aperiodically unsteady asymmetric configuration of two or more vortices appears. Although adequate for dividing the flow into steady and unsteady regimes, these simple classifications are not always indicative of the vortex configuration over the entire length of the body since the configuration varies with distance downstream from the nose of the model.

For angles of attack less than approximately 22°, a symmetric pair of steady oppositely rotating vortices is formed on the upper side of the body. These vortices, which were first detected near the base of the model, were not found with the vapor-screen technique for angles of attack less than 6°. However, it is known from the pressure distributions to be discussed later that cross-flow separation with presumed formation of the vortices occurred at even smaller angles of attack. As the angle of attack is increased above 6°, the vortices appear to increase in strength and may be traced progressively farther forward on the body so that at approximately 15°, they extend over the entire length of the body.

The angle-of-attack range in which a steady asymmetric configuration of two vortices appears is from approximately 22° to 26°. The asymmetry is first detected near the base of the model so that while the vortex pattern is asymmetric near the base, it may be symmetric over the forward part of the model. With increase in angle of attack within this range, the asymmetry becomes more pronounced and, at approximately 26°, the flow becomes unsteady.

For all angles of attack from approximately 26° to 36°, the maximum angle of attack of the tests, the aperiodically unsteady configuration of two or more vortices appears. The vortex configuration is similar to that shown by the vapor screen and schlieren pictures of figure 2 in which the pattern of vortices near the base, figure 2(c), resembles the familiar Kármán vortex street. Two different unsteady configurations are found in this angle-of-attack range. One is associated with the appearance of an additional vortex in the flow field and the other with a simple shifting of the asymmetry of the vortex pattern. In either case these changes occur aperiodically with no apparent change in either the angle of attack or the free-stream flow conditions and are accompanied by a shuddering of the model, indicating a sudden change in force distribution.

It has been pointed out previously (ref. 3) that there is an analogy between the development of the cross-flow vortex system with distance along an inclined body and the development with time of the flow about a circular cylinder set in motion impulsively from rest in a direction normal to the axis of revolution. In both flows a pair of symmetric vortices is developed initially. These vortices grow in size and are elongated in the cross-flow direction with distance along the body for the inclined body and with time elapsed for the circular cylinder. Eventually, this flow pattern becomes unstable and a periodic discharge of vortices results. For the inclined body, the periodic vortex discharge appears when the development of the flow is viewed in a plane which moves with the fluid; whereas for the circular cylinder, the periodicity appears when the flow is viewed in a plane which is fixed with respect to the cylinder.

Pressure Distributions

Zero lift.- The theoretical pressure distribution at zero angle of attack has been calculated by several different methods for comparison with the experimental data presented in figure 3. Since the slope of the surface of the body is everywhere small relative to the free-stream Mach angle, there is little difference between the results obtained by the use of the linear theory (ref. 6) and the more exact methods of the second-order theory or the method of characteristics, references 7 and 8, respectively. The principal difference in the theoretical results is in the pressure coefficient at the nose of the model. For this Mach number and nose angle, the second-order theory yields results which agree with the exact Taylor-Maccoll value; whereas the linear theory yields a somewhat lower value. The method of characteristics solution for the pressure distribution over the nose of this model was computed from the analytic expression given in reference 8. The expression results from the correlation of a number of characteristics solutions, and is expressed in terms of the hypersonic similarity parameter. Since it was necessary to extrapolate the results presented therein for the present application, the accuracy has undoubtedly suffered to some extent. Nevertheless, the agreement of this result with experiment may be considered adequate in view of the extreme simplicity of computation achieved by use of the simple equation. The corresponding distribution over the cylindrical afterbody was determined by cross-plotting values obtained from the appropriate figures of reference 8. The distributions calculated with linear theory and second-order theory coincide over most of the body length. These distributions were calculated only to a point approximately two body diameters aft of the point of tangency of the nose with the afterbody since the trend of the curves was clearly established, and the large amount of calculation necessary to obtain the distribution for the full body length was not considered justified.

The waviness of the experimental pressure distribution over the nose section has been attributed directly to irregularities of slope of the model surface. As determined by a contour projector, the magnitude of slope deviation from the theoretical was approximately 0.25° at $x = 2.7d$ and approximately 0.12° at $x = 1.4d$. The apparently low values of the pressure coefficients for $x/d<1$ are due to a slightly smaller nose angle on the model than was assumed for the theoretical calculations.

Angle of attack.- Although there are a number of theoretical methods for calculating the pressure distributions for inclined bodies of revolution (refs. 1 and 9 to 16, for example), the angles of attack and body shapes for which these methods might be expected to yield accurate results are limited. These limitations result from both the failure to consider the effects of viscosity and the assumption of small disturbances in the development of the theory.

Since the viscous effects are associated with separation of the cross flow and since separation would be expected only if the pressure gradient in the flow direction were adverse, a study of the theoretical inviscid pressure distributions should give some indication of the conditions for which cross-flow separation might be anticipated. In this regard, it is of interest to consider the variation with angle of attack of the position of the minimum pressure line as determined from the pressure distribution predicted by the following expression (refs. 1, 9, or 10):

$$\Delta C_p = 2 \frac{dr}{dx} \cos \theta \sin 2\alpha + \sin^2\alpha \, (1-4 \sin^2\theta)$$

As shown in figure 4, for all angles of attack other than zero, the theoretical minimum pressure line on the cylindrical afterbody is at $\theta = 90^{\circ}$. On the nose section of the body, as the angle of attack is increased from 0° to 90°, the minimum-pressure line moves progressively from $\theta = 180^{\circ}$ to $\theta = 90^{\circ}$. Although the cross-flow separation line would not be expected to coincide with the minimum-pressure line, it might be expected to follow the same trends. Hence, based upon the results shown in figure 4, cross-flow separation should occur initially on the cylindrical afterbody and should move forward with increasing angle of attack. That this expected trend is actually realized is illustrated by the typical pressure-distribution data in figure 5. The circumferential pressure distributions are shown for four angles of attack. The data for the station 11.33 diameters from the bow of the model indicate that at this station, the cross flow has separated at an angle of attack as low as 1°. With increasing angle of attack, the position along the body aft of which the cross flow has separated moves forward. Plots of the data appearing in table I show that at approximately 15°, the cross flow has separated over the entire body length. The position along the body at which cross-flow separation first occurs is plotted as a function of angle of attack in figure 6.

It is within this separated-flow region that the vortices which were observed with the aid of the vapor-screen technique are formed. The secondary flow of these vortices has pronounced effects on the local distribution of pressure within the separated-flow region. These effects are predominant in the lower angle-of-attack range where the vortices are close to the surface of the body. The low pressure region near $\theta = 150^{\circ}$ (figs. 5(c) and 5(d), for example) is associated with the location of a vortex core. The higher pressure which occurs in the plane of symmetry on the lee side ($\theta = 180^{\circ}$) results from the combined effects of the two symmetrically situated vortices which rotate in opposite directions and tend to produce a quasi-stagnation line along the body surface. The variation with distance along the body of the effect of the vortex pair on the local pressure distribution is illustrated by the data shown in figure 5(d). The magnitude of the expected pressure rise at $\theta = 180^{\circ}$ is proportional to the strength of the vortices and inversely proportional to their distance from the body surface. Over the nose where the vortices were weak, but still close to the body, a small pressure rise is shown. At station 6.67d the combination of vortex strength and location was such that the largest pressure rise occurred at this station. At stations farther downstream the effect of the vortices was less, and at station $x = 11.33d$ the pressure was nearly constant because the vortices were so far from the body that in spite of their increased strength, they had little local influence on the body pressure.

Although it is apparent from the foregoing that viscous effects are important even at low angles of attack, it is evident that the region of influence of these viscous effects is confined principally to the lee side of the body. Hence, the pressure distribution for the remainder of the body might be adequately predicted by potential theory. For comparison with the experimental results, the pressure distributions predicted by slender-body theory (ref. 1) have been plotted in figure 5 for several stations along the body. These particular stations were chosen for the comparisons since they are representative of the three different flow regions of the body. The first station is on the expanding portion, the second and third stations are within the region of lift carry-over on the cylindrical afterbody, and the fourth station is sufficiently far along the cylindrical portion of the body so that it should be influenced very little by the lift carry-over from the nose. At the lowest angle of attack the magnitude of the lifting pressure coefficients is so small relative to the uncertainty in the measurements that comparisons with the theoretical distributions have little significance. For low angles of attack where the effects of cross-flow separation are not evidenced, the experimental pressure distributions for the station on the nose of the body are in good agreement with the theory on both the windward and leeward sides. For the balance of the stations the agreement is generally poor for angles of attack of 0.9° and 4.0°. However, for 8°, fair agreement over most of the windward side of the model is found.

For angles of attack greater than 10° the Mach number normal to the inclined axis of the body exceeds the well-known critical cross-flow Mach number for a circular cylinder. Hence, it might be anticipated that for this and larger angles of attack, compressibility effects would contribute to the lack of agreement of the experimental pressure distributions with those predicted by the theory. The pressure-distribution data show that this compressibility effect results in larger pressures than predicted over the windward side of the model. At 15° angle of attack this compressibility effect is not constant along the body length; instead, the difference between the experiment and theory on the windward side diminishes with distance along the body, and at $x = 11.33d$ the experimental distribution is in good agreement with the incompressible theory. However, as the angle of attack is increased above 15°, the circumferential distributions over the cylindrical portion of the body become less dependent upon axial position. The variation with angle of attack at stations along the cylindrical afterbody in this high angle-of-attack range is shown in figure 7. At approximately 29.5° angle of attack, or a cross Mach number of 1.0, the circumferential pressure distributions are almost identical over the entire cylindrical afterbody and thus depend only on the cross-stream characteristics. As shown by the data in figure 7, at high angles of attack the pressure distribution over the windward side of the body approaches that predicted by classical Newtonian theory (ref. 14), although, as would be expected, the pressures are all somewhat lower than the Newtonian values. The level of the pressure in the wake (fig. 7) decreases with increasing angle of attack. At $\alpha = 35.5^{\circ}$, the pressure over most of the lee side of the body is constant and the pressure coefficient is equal to approximately 0.7 of that corresponding to a vacuum. It is interesting to note that the pressure level is very close to the minimum pressure on the lee side of a cylinder in two-dimensional flow at the same free-stream Mach number (ref. 17). Hence, it appears that the lee-side pressure for the inclined body may have already reached a lower limit at the maximum angle of attack of these tests and would therefore not decrease with further increases in incidence.

Lift Distribution

Theory.- In the analysis of reference 2, it was assumed that the viscous cross flow about an inclined body of revolution is similar to that about a circular cylinder normal to an air stream of velocity

$V_o \sin \alpha$. Thus, the local cross force resulting from the effects of viscosity could be computed from a knowledge of the drag characteristics of circular cylinders. It was further assumed that this so-called viscous cross force could be added directly to the local cross force resulting from the potential flow. Based upon these assumptions, expressions for the lift, drag rise, and moment were developed as functions of the angle of attack. It is the purpose of the following section to examine the experimental lift distribution and center-of-pressure location in light of this theory.

Comparison of theory and experiment.- The experimental longitudinal distribution of local normal-force coefficient for model 2 is compared with theoretical distributions in figure 8 for several angles of attack. Munk's slender-body theory (ref. 18) and Tsien's linearized theory (ref. 13) have each been combined with the so-called viscous cross force calculated in accordance with reference 2 to yield two different theoretical distributions. The theoretical viscous cross-flow contribution has also been shown separately. Insofar as the absolute magnitude of the local cross-force coefficients at angles of attack of 1° and 2° is concerned, the small difference between the two theoretical results is somewhat overshadowed by the uncertainty in the experimental data, thus precluding a selection of the better theory on this basis alone. However, in this low angle range the linearized theory does predict the general trends of the experimental data better than the slender-body theory. In particular, the negative lift region on the cylindrical afterbody is indicated, although neither the exact location nor magnitude of the maximum negative lift is correctly predicted. For the highest angle-of-attack data of figure 8, there is little semblance between theory and experiment except over the first three or four body diameters.

The local normal-force data for model 1 presented in figure 9 afford an opportunity to assess the validity of two of the assumptions of the approximate method of reference 2. These two assumptions were: First, that the cross-flow drag coefficient used for calculating the local cross force on each element of an inclined body was constant along the length of the body; and second, that the appropriate magnitude of the cross-flow drag coefficient should be the two-dimensional value reduced by a factor to account for the finite length of the body.[2] Thus, in the approximate method, the cross force on each element of the body was

[2]This suggestion was made since it was known that the drag coefficient of a circular cylinder of finite length was less than the drag coefficient of a circular cylinder of infinite length. Although it was recognized that the largest portion of the drag reduction due to finite length should occur near the ends of the body, it was expedient to consider the drag reduction to be equal for each element along the length of the body.

reduced by the factor η which is the ratio of the drag of a circular cylinder of finite length to that of a circular cylinder of infinite length. Since, for the angle-of-attack range of the data of figure 9, the major contribution to the local normal force over the cylindrical afterbody results from the cross-flow separation forces, the validity of these assumptions can be assessed. As to the assumed constancy of the cross-flow drag coefficient, only at the highest angle of attack is the cross force constant over the afterbody length. For the angle-of-attack range between 10° and 20° the normal force decreases continuously with distance downstream from the beginning of the cylindrical afterbody. Although the cross force does vary with distance along the body, the nature of the distributions indicates that for each angle of attack, the cross force is approaching a constant value far downstream. However, this asymptotic value is not reached on the body for angles of attack less than about 20°. For angles of attack of 24.5° and greater, the cross force is constant over a portion of the afterbody. It appears, therefore, that for all but the largest angles of attack the cross-force distribution on the cylindrical afterbody is influenced by the presence of the nose of the body and that the length of afterbody influenced by this end effect decreases as the angle of attack increases. Hence, the assumption of reference 2 that the cross-flow drag coefficient is constant along the length of the afterbody is most appropriate for very large angles of attack.

The second assumption of reference 2 that may be examined is that of the appropriate magnitude of the cross-flow drag coefficient. The dashed lines shown in figure 9 represent the magnitude of the local normal-force coefficient calculated with the section drag coefficient for infinitely long circular cylinders ($\eta = 1$) for the appropriate cross Mach numbers and cross Reynolds numbers. These values, rather than the reduced values suggested in reference 2 ($\eta \cong 0.76$), are shown since the reduced values yielded results which were, in general, too low over most of the length of the cylindrical afterbody. From these comparisons it is apparent that neither the reduced values nor the values represented by the dashed lines in figure 9 are appropriate for the complete angle-of-attack range. It was conjectured in reference 2 that the value of η for cross Mach numbers other than that for which data were available ($M \rightarrow 0$) could be estimated by considering the effective length-to-diameter ratio as proportional to the true length-to-diameter ratio multiplied by the ratio of the drag coefficient, 1.2, to the section drag coefficient at the Mach number under consideration. Thus, as the cross Mach number increased in the subsonic range, the value of η would decrease. However, it appears from the data of figure 9 that it would be more appropriate to consider that η approaches unity as the normal Mach number approaches unity. This is further supported by the results presented in references 17 and 19 wherein it was shown that η is effectively unity for supersonic cross Mach numbers.

An effect of Reynolds number.- An effect of Reynolds number on the local cross force is indicated by the comparison in figure 8(e) of the local cross-force distribution on the cylindrical afterbodies of models 1 and 2 for an angle of attack of 15.1°. These data show that the local cross force over the aft portion of the afterbody of model 2 is much less than that for model 1.[3] Although the two sets of experimental data were obtained for identical free-stream conditions, the difference in size of the two models results in a difference in the Reynolds number based on model dimensions. This loss in cross force for model 2 appears to be similar in nature to the reduction in cross force or drag of a circular cylinder which occurs when the critical Reynolds number is exceeded. For this latter case, the reduction in drag results from transition of the boundary layer on the cylinder which alters the separation point and effects an increase in the pressure recovery on the lee side of the body. Comparison of the circumferential pressure distributions at $x = 14d$ for models 1 and 2 with typical pressure distributions for the subcritical and supercritical Reynolds number flow around a circular cylinder (fig. 10) shows that the differences between the distributions for models 1 and 2 are similar to the differences between the distributions for the circular cylinder.[4] An increase of Reynolds number results in a larger pressure recovery on the leeward side of the body and a lower minimum pressure which occurs nearer $\theta = 90^{\circ}$.

Two significant facts concerning the values of the cross-flow Mach number and the Reynolds number at which this effect was found should be noted. The cross-flow Mach number was approximately 0.5 which is greater than the critical Mach number for a circular cylinder. Thus, it is apparent that contrary to expectations, the critical cross-flow Mach number for a circular cylinder ($M = 0.4$) is not the maximum cross Mach number for which Reynolds number effects can be important. However, this result does not imply that the Reynolds number will have important effects for all cross Mach numbers since it is obvious that if the cross-flow separation characteristics are primarily dependent on shock-wave boundary-layer interaction, as they must be for large cross Mach numbers, the Reynolds number should have little effect. The second significant result is that the cross-flow Reynolds number, based upon the velocity normal to the inclined axis and the afterbody diameter of model 2, was less than the familiar critical cross-flow Reynolds number for a circular cylinder. This result is in agreement with the results of reference 19 which show that the critical Reynolds number for the flow about a circular cylinder inclined to the air stream is less than the critical Reynolds

[3]To provide a direct comparison of the local normal-force distribution of models 1 and 2, the experimental data for model 1, as plotted in figure 8, have been referred to the dimensions of model 2 since, by definition (see list of symbols), the local normal-force coefficient has the dimensions r^{-1}.

[4]The reference q used for this plot is the q normal to the axis of revolution ($q_o \sin^2\alpha$).

number based upon the local diameter of the body, and the velocity normal to the axis of the body. Thus, the cross-flow Reynolds number may not be the proper parameter for correlating transition effects on the cross force for inclined bodies. In this regard, it should be noted that for model 2 of the present investigation, the Reynolds number, based upon the free-stream velocity and the distance from the nose of the model to the axial position at which the transition effects on the cross flow were first detected, was near the value for which transition of the longitudinal boundary layer would be expected for the test conditions and within this particular wind tunnel. Thus, transition of the longitudinal boundary layer may have contributed to the apparently low value of the critical cross-flow Reynolds number.

Lift and Moment Characteristics

The pressure-distribution data for model 2 have been integrated to determine lift and moment characteristics. To provide a direct comparison with force data obtained from previous tests of a model with an identical ogival nose but of over-all fineness ratio of 13.1, the integrations were terminated at $x = 13.1d$. The comparison of these results is shown in figures 11 and 12. Also included in the figures are the characteristics predicted with potential theory alone and with both slender-body theory and Tsien's linearized theory in combination with estimates of the viscous effects. The viscous contribution has been estimated by both the method suggested in reference 2 in which the reduced value of the cross-flow drag coefficient is used ($\eta = 0.72$) and by assuming the full value of the cross-flow drag coefficient to be effective ($\eta = 1.0$). The use of Tsien's linearized theory in place of slender-body theory has little effect on moment and center of pressure. Some slight improvement in the prediction of the lift and pitching moment at the higher angles of attack results from use of the full value of the cross-flow drag coefficient, but this is accompanied by a loss in agreement in the low angle-of-attack range.

CONCLUDING REMARKS

The pressure distribution and force characteristics of a slender body of revolution consisting of a fineness ratio 5.75, circular-arc, ogival nose tangent to a cylindrical afterbody have been measured for an angle-of-attack range of 0° to approximately 36°. The free-stream Reynolds number and Mach number were 0.5×10^6 per inch and 1.98, respectively. Comparisons of the results with theory show that the pressure distribution over the nose of the body is adequately predicted for low angles of attack. Viscous effects which result in separation of the cross flow caused considerable disagreement over the aft leeward side of the cylindrical afterbody even at very low angles of attack. The cross-flow-separation point (the position on the body aft of which the cross flow is separated) moved forward with increasing angle of attack, with the result that the cross flow is separated for the entire length of the body at an angle of attack of 15.1°.

The results of the study of the cross-force distribution have shown that even though the total cross force or lift is in fair agreement with that predicted by the approximate method proposed by Allen (NACA RM A9I26), the distribution of loading differs appreciably from that assumed in the analysis. It is not possible to determine from the present tests if the differences between the experimental results and the various theories may be attributed to failure of the potential-flow theory or to viscous effects which have not been taken into account. However, because of the nature of these differences, it appears that they result largely from the viscous effects. Additional theoretical and experimental work is needed to explore the possible relationship between the time dependency of the viscous forces for the circular cylinder impulsively set in motion from rest and the axial distribution of the viscous forces for the inclined body, which is suggested by the analogy between the development with time of the flow about the circular cylinder and the development with distance of the flow along the inclined body.

An effect of Reynolds number on the cross flow about the inclined body was found. The effect was similar to that which occurs for the two-dimensional flow around a circular cylinder when the Reynolds number exceeds the well-known critical value. Two significant facts about this effect should be noted. The cross-flow Reynolds number at which the reduction in cross force occurred was less than the familiar critical value for a circular cylinder normal to the air stream. The cross Mach number was greater than the critical Mach number for a circular cylinder. Thus, it appears that the critical cross-flow Reynolds number for the flow around the inclined body is less than that of a circular cylinder normal to the air stream, and that Reynolds number effects are important even at cross Mach numbers greater than the critical Mach number for a circular cylinder.

Ames Aeronautical Laboratory
National Advisory Committee for Aeronautics
Moffett Field, Calif., May 1, 1953

REFERENCES

1. Allen, H. Julian: Pressure Distribution and some Effects of Viscosity on Slender Inclined Bodies of Revolution. NACA TN 2044, 1950.

2. Allen, H. Julian: Estimation of the Forces and Moments Acting on Inclined Bodies of Revolution of High Fineness Ratio. NACA RM A9I26, 1949.

3. Allen, H. Julian, and Perkins, Edward W.: Characteristics of Flow Over Inclined Bodies of Revolution. NACA RM A50L07, 1951.

4. Perkins, Edward W., Gowen, Forrest E., and Jorgensen, Leland H.: Aerodynamic Characteristics of the NACA RM-10 Research Missile in the Ames 1- by 3-Foot Supersonic Wind Tunnel No. 2 - Pressure and Force Measurements at Mach Numbers of 1.52 and 1.98. NACA RM A51G13, 1951.

5. Perkins, Edward W., and Jorgensen, Leland H.: Comparison of Experimental and Theoretical Normal-Force Distributions (Including Reynolds Number Effects) on an Ogive-Cylinder Body at Mach Number 1.98. NACA TN 3716, 1956. (Formerly NACA RM A54H23)

6. von Kármán, Theodor, and Moore, Norton B.: Resistance of Slender Bodies Moving with Supersonic Velocities with Special Reference to Projectiles. Trans. ASME, vol. 54, no. 23, Dec. 15, 1932, pp. 303-310.

7. Van Dyke, Milton D.: A Study of Second-Order Supersonic-Flow Theory. NACA Rep. 1081, 1952. (Formerly NACA TN 2200)

8. Ehret, Dorris M., Rossow, Vernon J., and Stevens, Victor I., Jr.: An Analysis of the Applicability of the Hypersonic Similarity Law to the Study of Flow about Bodies of Revolution at Zero Angle of Attack. NACA TN 2250, 1950.

9. Luidens, Roger W., and Simon, Paul C.: Aerodynamic Characteristics of NACA RM-10 Missile in the 8- by 6-Foot Supersonic Wind Tunnel at Mach Numbers from 1.49 to 1.98. I - Presentation and Analysis of Pressure Measurements (Stabilizing Fins Removed). NACA RM E50D10, 1950.

10. Lighthill, M. J.: Supersonic Flow Past Slender Pointed Bodies of Revolution at Yaw. Quart. Jour. Mech. and Appl. Math., vol. 1, pt. 1, March 1948, pp. 76-89.

11. Laitone, E. V.: The Linearized Subsonic and Supersonic Flow About Inclined Slender Bodies of Revolution. Jour. Aero. Sci., vol. 14, no. 11, Nov. 1947, pp. 631-642.

12. Ward, G. N.: Supersonic Flow Past Slender Pointed Bodies. Quart. Jour. Mech. and Appl. Math., vol. 2, pt. 1, March 1949, pp. 75-97.

13. Tsien, Hsue-Shen: Supersonic Flow Over an Inclined Body of Revolution. Jour. Aero. Sci., vol. 5, no. 12, Oct. 1938, pp. 480-483.

14. Grimminger, G., Williams, E. P., and Young, G. B. W.: Lift on Inclined Bodies of Revolution in Hypersonic Flow. Jour. Aero. Sci., vol. 17, no. 11, Nov. 1950, pp. 675-690.

15. Kaplan, Carl: Potential Flow about Elongated Bodies of Revolution. NACA Rep. 516, 1935.

16. Ferri, Antonio: The Method of Characteristics for the Determination of Supersonic Flow over Bodies of Revolution at Small Angles of Attack. NACA Rep. 1044, 1951. (Formerly NACA TN 1809)

17. Gowen, Forrest E., and Perkins, Edward W.: Drag of Circular Cylinders for a Wide Range of Reynolds Numbers and Mach Numbers. NACA TN 2960, 1953. (Formerly NACA RM A52C20)

18. Munk, Max M.: The Aerodynamic Forces on Airship Hulls. NACA Rep. 184, 1924.

19. Bursnall, William J., and Loftin, Laurence K., Jr.: Experimental Investigation of the Pressure Distribution about a Yawed Circular Cylinder in the Critical Reynolds Number Range. NACA TN 2463, 1951.

TABLE I.- EXPERIMENTAL PRESSURE COEFFICIENTS FOR A 33-1/3-CALIBER OGIVE-CYLINDER MODEL AT VARIOUS ANGLES OF ATTACK. $M_o = 1.98$, $Re_o = 0.5 \times 10^6$/INCH, MODEL 1

(a) $\alpha = 10.5^o$

$\frac{x}{d}$	Radial angle, θ																			
	0°	15°	30°	45°	60°	90°	105°	120°	135°	150°	180°	195°	210°	225°	240°	270°	285°	300°	315°	330°
6.08	0.058	0.051	0.008	-0.037	-0.076	-0.139	-0.125	-0.090	-0.060	-0.049	-0.039	-0.075	-0.070	-0.063	-0.096	-0.146	-0.108	-0.068	-0.035	0.009
6.74	.037	.028	.006	-.039	-.079	—	—	—	—	—	-.027	-.049	-.043	-.077	-.096	-.135	-.117	-.076	-.040	.006
7.41	.036	.029	.006	-.043	-.083	-.137	-.120	-.087	-.057	-.045	-.028	-.040	-.042	-.043	-.080	-.121	-.115	-.078	-.044	.003
8.08	.035	.026	0	-.049	-.088	-.124	-.097	-.053	-.055	-.045	-.023	-.045	-.048	-.071	-.049	—	—	—	—	—
8.75	—	—	—	—	—	-.112	-.076	-.040	-.052	-.053	-.021	-.030	-.074	-.047	-.054	-.100	-.105	-.082	-.031	-.001
9.41	.027	.019	-.006	-.036	-.064	-.097	-.062	-.032	-.046	-.050	-.017	-.033	-.037	-.044	-.031	-.090	-.094	-.082	-.037	-.003
10.08	.025	.019	-.007	-.032	-.074	-.084	-.038	-.031	-.045	-.054	-.017	-.032	-.033	-.044	-.033	—	—	—	—	—
10.75	.029	.015	-.006	-.046	-.073	-.078	-.041	-.033	-.042	-.076	-.018	-.021	-.045	-.040	-.053	-.072	-.081	-.076	-.035	-.013
11.41	.032	.023	-.003	-.034	-.069	-.070	-.030	-.029	-.032	-.046	-.012	-.029	-.038	-.033	-.038	-.060	-.072	-.065	-.032	.002
12.08	.032	.020	0	-.029	-.062	-.068	-.030	-.029	-.028	-.037	-.013	-.032	-.031	-.030	-.032	—	—	—	—	—
12.75	.029	.021	0	-.038	-.062	-.069	-.033	-.033	-.030	-.036	-.015	-.063	-.031	-.030	-.035	-.065	-.077	-.068	-.035	-.008
13.41	.041	.034	.011	-.086	-.065	-.063	-.044	-.041	-.032	-.036	-.017	-.046	-.041	-.026	-.035	-.048	-.051	-.049	-.026	.007
14.08	.044	.033	.009	-.087	-.065	-.067	-.044	-.037	-.028	-.031	-.018	-.045	-.047	-.028	-.029	—	—	—	—	—
14.75	—	—	—	—	—	-.070	-.033	-.031	-.029	-.035	-.023	-.041	-.039	-.026	-.022	-.046	-.061	-.050	-.021	.014
15.41	.035	.030	.006	-.029	-.069	-.065	-.036	-.027	-.027	-.032	-.018	-.035	-.025	-.024	-.029	-.046	-.063	-.058	-.024	.010
16.08	.031	.030	.006	-.027	-.067	-.058	-.036	-.027	-.026	-.029	-.018	-.032	-.021	-.022	-.021	—	—	—	—	—
16.75	.027	.025	.005	-.029	-.064	-.078	-.038	-.029	-.029	-.031	-.019	-.029	-.020	-.020	-.022	-.054	-.067	-.060	-.027	.002

(b) $\alpha = 14.5^o$

$\frac{x}{d}$	Radial angle, θ																			
	0°	15°	30°	45°	60°	90°	105°	120°	135°	150°	180°	195°	210°	225°	240°	270°	285°	300°	315°	330°
6.08	0.076	0.060	0.087	-0.026	-0.082	-0.158	-0.134	-0.120	-0.134	-0.110	-0.066	-0.074	-0.115	-0.114	-0.114	-0.150	-0.128	-0.067	-0.012	0.032
6.74	.073	.058	.021	-.031	-.089	—	—	—	—	—	-.057	-.074	-.105	-.110	-.111	-.124	-.136	-.078	-.082	.028
7.41	.072	.055	.018	-.036	-.095	-.120	-.107	-.116	-.128	-.117	-.051	-.062	-.109	-.108	-.104	-.118	-.153	-.082	-.084	.026
8.08	.067	.058	.013	-.042	-.097	-.109	-.086	-.082	-.109	-.121	-.048	-.068	-.106	-.098	-.074	—	—	—	—	—
8.75	—	—	—	—	—	-.096	-.079	-.062	-.099	-.111	-.043	-.081	-.088	-.082	-.063	-.107	-.096	-.090	-.032	.018
9.41	.065	.047	.009	-.045	-.090	-.087	-.080	-.065	-.089	-.094	-.045	-.100	-.067	-.071	-.067	-.106	-.083	-.091	-.036	.026
10.08	.061	.047	.010	-.043	-.090	-.087	-.072	-.083	-.084	-.073	-.047	-.111	-.060	-.079	-.072	—	—	—	—	—
10.75	.065	.051	.012	-.036	-.089	-.087	-.090	-.070	-.083	-.036	-.045	-.102	-.079	-.049	-.068	-.106	-.083	-.090	-.038	.014
11.41	.060	.046	.010	-.029	-.086	-.095	-.071	-.061	-.071	-.065	-.042	-.084	-.063	-.061	-.060	-.103	-.118	-.079	-.031	.015
12.08	.061	.049	.013	-.028	-.085	-.103	-.078	-.061	-.067	-.056	-.046	-.054	-.070	-.077	-.069	—	—	—	—	—
12.75	.065	.038	.014	-.088	-.082	-.108	-.088	-.061	-.043	-.071	-.049	-.052	-.045	-.053	-.064	-.112	-.129	-.080	-.074	.016
13.41	.067	.053	.016	-.080	-.088	-.095	-.078	-.064	-.059	-.065	-.041	-.052	-.039	-.065	-.072	-.072	-.104	-.088	-.080	.023
14.08	.068	.033	.014	-.034	-.089	-.084	-.065	-.060	-.054	-.064	-.047	-.055	-.060	-.062	-.046	—	—	—	—	—
14.75	—	—	—	—	—	-.081	-.041	-.044	-.072	-.077	-.046	-.046	-.049	-.074	-.037	-.076	-.111	-.073	-.083	.022
15.41	.064	.050	.014	-.033	-.087	-.078	-.040	-.039	-.063	-.063	-.046	-.040	-.044	-.064	-.036	-.076	-.110	-.074	-.026	.020
16.08	.064	.049	.014	-.032	-.085	-.078	-.044	-.042	-.045	-.045	-.046	-.039	-.042	-.039	-.040	—	—	—	—	—
16.75	.066	.050	.016	-.032	-.084	-.080	-.050	-.046	-.043	-.045	-.048	-.038	-.039	-.038	-.041	-.081	-.115	-.075	-.088	.028
17.41	.066	.053	.018	-.032	-.079	-.075	-.043	-.041	-.050	-.050	-.045	-.043	-.042	-.052	-.042	-.065	-.076	-.078	-.080	.027
18.08	.067	.052	.014	-.034	-.082	-.072	-.040	-.035	-.049	-.051	-.035	-.054	-.043	-.036	-.034	—	—	—	—	—
18.75	—	—	—	—	—	-.079	-.043	-.031	-.049	-.046	-.043	-.046	-.042	-.037	-.030	-.083	-.084	-.076	-.080	.027
19.41	.063	.051	.017	-.053	-.084	-.088	-.070	-.033	-.039	-.041	-.043	-.042	-.041	-.036	-.029	-.090	-.093	-.078	-.084	.024
20.08	.062	.049	.016	-.037	-.086	-.082	-.038	-.038	-.038	-.042	-.039	-.035	-.040	-.035	-.034	—	—	—	—	—
20.75	.063	.051	.019	-.052	-.088	-.088	-.062	-.041	-.036	-.043	-.041	-.036	-.037	-.053	-.036	-.102	-.108	-.082	-.086	.021

(c) $\alpha = 16.5^o$

$\frac{x}{d}$	Radial angle, θ																			
	0°	15°	30°	45°	60°	90°	105°	120°	135°	150°	180°	195°	210°	225°	240°	270°	285°	300°	315°	330°
6.08	0.122	0.098	0.056	-0.009	-0.079	-0.150	-0.138	-0.142	-0.150	-0.148	-0.087	-0.106	-0.144	-0.136	-0.143	-0.148	-0.136	-0.061	0.008	0.066
6.74	.112	.096	.051	-.015	-.087	—	—	—	—	—	-.084	-.106	-.138	-.126	-.125	-.131	-.140	-.067	-.002	.058
7.41	.109	.090	.046	-.021	-.092	-.120	-.126	-.124	-.139	-.148	-.067	-.115	-.134	-.136	-.126	-.130	-.136	-.078	-.009	.054
8.08	.100	.086	.042	-.027	-.097	-.110	-.094	-.090	-.132	-.136	-.064	-.130	-.121	-.116	-.097	—	—	—	—	—
8.75	—	—	—	—	—	-.099	-.074	-.086	-.133	-.123	-.070	-.133	-.096	-.108	-.081	-.114	-.102	-.081	-.017	.045
9.41	.096	.078	.035	-.030	-.101	-.092	-.086	-.108	-.128	-.096	-.023	-.126	-.088	-.088	-.087	-.110	-.096	-.088	-.085	.038
10.08	.092	.078	.030	-.031	-.100	-.098	-.092	-.107	-.097	-.076	-.054	-.110	-.067	-.066	-.066	—	—	—	—	—
10.75	.092	.074	.032	-.034	-.101	-.108	-.099	-.094	-.087	-.089	-.046	-.096	-.090	-.071	-.084	-.114	-.102	-.096	-.033	.028
11.41	.090	.073	.024	-.025	-.100	-.099	-.089	-.080	-.063	-.073	-.043	-.075	-.073	-.069	-.078	-.109	-.139	-.083	-.088	.035
12.08	.090	.074	.029	-.025	-.098	-.098	-.075	-.079	-.054	-.063	-.049	-.073	-.069	-.087	-.079	—	—	—	—	—
12.75	.088	.074	.030	-.030	-.102	-.097	-.081	-.075	-.049	-.065	-.058	-.076	-.070	-.080	-.076	-.103	-.126	-.093	-.032	.025
13.41	.098	.080	.030	-.032	-.104	-.100	-.080	-.092	-.089	-.118	-.054	-.077	-.086	-.086	-.069	-.080	-.131	-.085	-.029	.042
14.08	.096	.078	.030	-.034	-.101	-.091	-.065	-.071	-.081	-.110	-.055	-.076	-.082	-.078	-.050	—	—	—	—	—
14.75	—	—	—	—	—	-.085	-.072	-.059	-.078	-.095	-.061	-.065	-.076	-.063	-.044	-.067	-.118	-.080	-.019	.040
15.41	.092	.074	.028	-.032	-.097	-.079	-.058	-.070	-.087	-.093	-.060	-.056	-.062	-.070	-.048	-.064	-.122	-.064	-.028	.036
16.08	.090	.074	.030	-.036	-.095	-.077	-.053	-.071	-.058	-.066	-.061	-.050	-.060	-.044	-.071	—	—	—	—	—
16.75	.087	.070	.027	-.029	-.098	-.082	-.077	-.069	-.055	-.068	-.062	-.064	-.060	-.048	-.049	-.072	-.104	-.064	-.031	.026
17.41	.098	.081	.032	-.032	-.091	-.083	-.069	-.063	-.076	-.078	-.064	-.082	-.051	-.070	-.054	-.076	-.104	-.089	-.012	.046
18.08	.097	.079	.029	-.033	-.093	-.086	-.062	-.069	-.073	-.066	-.058	-.069	-.058	-.072	-.039	—	—	—	—	—
18.75	—	—	—	—	—	-.099	-.064	-.047	-.064	-.068	-.058	-.060	-.067	-.074	-.040	-.090	-.093	-.088	-.016	.043
19.41	.093	.073	.031	-.031	-.092	-.101	-.067	-.038	-.070	-.066	-.055	-.049	-.064	-.050	-.042	-.095	-.097	-.098	-.019	.039
20.08	.092	.074	.032	-.029	-.092	-.106	-.064	-.036	-.046	-.061	-.054	-.047	-.058	-.051	-.046	—	—	—	—	—
20.75	.088	.071	.028	-.034	-.098	-.109	-.062	-.036	-.051	-.063	-.057	-.050	-.058	-.062	-.053	-.098	-.096	-.095	-.086	.068

(d) $\alpha = 19.5^o$

$\frac{x}{d}$	Radial angle, θ																			
	0°	15°	30°	45°	60°	90°	105°	120°	135°	150°	180°	195°	210°	225°	240°	270°	285°	300°	315°	330°
6.08	0.184	0.159	0.102	0.025	-0.064	-0.158	-0.168	-0.163	-0.166	-0.180	-0.180	-0.182	-0.175	-0.167	-0.162	-0.175	-0.132	-0.044	0.042	0.116
6.74	.178	.156	.096	.020	-.070	—	—	—	—	—	-.099	-.176	-.167	-.162	-.150	-.161	-.132	-.073	.034	.104
7.41	.177	.153	.092	.015	-.078	-.136	-.146	-.139	-.164	-.165	-.092	-.162	-.154	-.155	-.144	-.152	-.143	-.062	.086	.104
8.08	.170	.149	.088	.008	-.082	-.132	-.122	-.126	-.158	-.157	-.087	-.156	-.150	-.141	-.120	—	—	—	—	—
8.75	—	—	—	—	—	-.126	-.127	-.137	-.143	-.140	-.088	-.144	-.138	-.126	-.124	-.138	-.150	-.068	.015	.094
9.41	.158	.136	.078	-.001	-.086	-.127	-.130	-.132	-.131	-.128	-.081	-.135	-.137	-.120	-.115	-.132	-.151	-.076	.008	.084
10.08	.154	.134	.076	-.002	-.088	-.128	-.129	-.128	-.130	-.124	-.075	-.135	-.134	-.128	-.119	—	—	—	—	—
10.75	.144	.128	.072	-.006	-.092	-.128	-.121	-.120	-.128	-.131	-.071	-.136	-.135	-.123	-.114	-.132	-.128	-.090	-.009	.068
11.41	.151	.130	.074	-.005	-.092	-.109	-.123	-.111	-.109	-.124	-.072	-.123	-.128	-.109	-.116	-.128	-.136	-.081	.003	.082
12.08	.149	.127	.073	-.006	-.090	-.110	-.115	-.106	-.096	-.121	-.073	-.123	-.130	-.123	-.111	—	—	—	—	—
12.75	.140	.121	.068	-.011	-.093	-.113	-.112	-.107	-.096	-.128	-.075	-.129	-.136	-.127	-.109	-.123	-.135	-.094	-.014	.067
13.41	.162	.134	.073	-.008	-.095	-.101	-.107	-.114	-.124	-.140	-.074	-.118	-.118	-.116	-.095	-.098	-.144	-.064	.006	.084
14.08	.159	.135	.074	-.009	-.096	-.103	-.084	-.099	-.110	-.126	-.092	-.098	-.114	-.101	-.064	—	—	—	—	—
14.75	—	—	—	—	—	-.106	-.085	-.087	-.098	-.109	-.083	-.106	-.112	-.087	-.083	-.094	-.134	-.025	.004	.082
15.41	.150	.126	.068	-.011	-.097	-.106	-.096	-.108	-.098	-.103	-.082	-.094	-.104	-.079	-.082	-.097	-.133	-.098	-.002	.093
16.08	.147	.123	.066	-.011	-.096	-.110	-.103	-.106	-.089	-.100	-.080	-.098	-.108	-.099	-.099	—	—	—	—	—
16.75	.139	.116	.061	-.014	-.098	-.119	-.157	-.103	-.090	-.106	-.081	-.107	-.117	-.122	-.104	-.098	-.108	-.096	-.015	.078
17.41	.150	.133	.069	-.013	-.094	-.106	-.101	-.087	-.101	-.104	-.094	-.104	-.098	-.104	-.078	-.089	-.112	-.090	.002	.081
18.08	.154	.133	.068	-.014	-.091	-.112	-.098	-.079	-.089	-.108	-.090	-.088	-.109	-.099	-.081	—	—	—	—	—
18.75	—	—	—	—	—	-.120	-.113	-.076	-.089	-.098	-.091	-.067	-.103	-.088	-.088	-.105	-.133	-.089	.003	.080
19.41	.116	.126	.066	-.012	-.088	-.124	-.124	-.089	-.066	-.076	-.089	-.080	-.089	-.081	-.095	-.108	-.133	-.089	-.008	.075
20.08	.144	.124	.063	-.010	-.086	-.120	-.120	-.096	-.074	-.073	-.087	-.078	-.089	-.096	-.103	—	—	—	—	—
20.75	.137	.119	.060	-.012	-.088	-.117	-.111	-.094	-.054	-.061	-.098	-.089	-.099	-.112	-.103	-.107	-.108	-.096	-.011	.061

TABLE I.- EXPERIMENTAL PRESSURE COEFFICIENTS FOR A 33-1/3-CALIBER OGIVE-CYLINDER MODEL AT VARIOUS ANGLES OF ATTACK. $M_o = 1.98$, $Re_o = 0.5 \times 10^6$/INCH, MODEL 1 - Continued

(e) $\alpha = 22.5^{\circ}$

$\frac{x}{d}$	Radial angle, θ																			
	0°	15°	30°	45°	60°	90°	105°	120°	135°	150°	180°	195°	210°	225°	240°	270°	285°	300°	315°	330°
6.08	0.236	0.234	0.137	0.060	-0.046	-0.193	-0.186	-0.188	-0.189	-0.198	-0.130	-0.216	-0.205	-0.196	-0.193	-0.219	-0.128	-0.083	0.079	0.171
6.74	.243	.220	.147	.072	-.072	—	—	—	—	—	-.139	-.214	-.200	-.191	-.188	-.216	-.136	-.094	.088	.163
7.41	.240	.214	.141	.045	-.057	-.168	-.166	-.169	-.186	-.194	-.130	-.209	-.192	-.183	-.177	-.200	-.145	-.097	.074	.148
8.08	.237	.212	.136	.039	-.062	-.160	-.162	-.165	-.176	-.184	-.128	-.201	-.188	-.177	-.168	—	—	—	—	—
8.75	—	—	—	—	—	-.152	-.163	-.159	-.166	-.169	-.124	-.194	-.184	-.168	-.169	-.182	-.147	-.090	.049	.141
9.41	.218	.194	.124	.032	-.069	-.151	-.162	-.150	-.162	-.162	-.119	-.187	-.176	-.169	-.160	-.180	-.153	-.096	.042	.151
10.08	.216	.198	.122	.031	-.068	-.147	-.152	-.152	-.170	-.165	-.115	-.181	-.168	-.159	-.154	—	—	—	—	—
10.75	.227	.194	.124	.034	-.067	-.148	-.155	-.144	-.163	-.162	-.116	-.176	-.163	-.158	-.148	-.160	-.158	-.084	.035	.134
11.41	.222	.186	.118	.027	-.073	-.143	-.153	-.146	-.142	-.157	-.136	-.179	-.164	-.163	-.148	-.158	-.157	-.082	.035	.136
12.08	.209	.185	.118	.028	-.073	-.147	-.152	-.148	-.152	-.164	-.141	-.165	-.158	-.149	-.154	—	—	—	—	—
12.75	.212	.187	.120	.030	-.069	-.156	-.143	-.152	-.154	-.164	-.141	-.158	-.151	-.155	-.148	-.161	-.156	-.083	.034	.121
13.41	.230	.185	.125	.028	-.070	-.170	-.159	-.136	-.156	-.158	-.154	-.156	-.159	-.158	-.146	-.157	-.163	-.066	.033	.126
14.08	.233	.193	.123	.025	-.073	-.175	-.160	-.138	-.148	-.151	-.145	-.142	-.157	-.139	-.146	—	—	—	—	—
14.75	—	—	—	—	—	-.179	-.162	-.160	-.143	-.147	-.150	-.138	-.144	-.137	-.141	-.154	-.154	-.063	.036	.130
15.41	.216	.182	.114	.022	-.076	-.176	-.174	-.155	-.142	-.136	-.150	-.133	-.138	-.144	-.142	-.117	-.146	-.057	.033	.120
16.08	.210	.180	.114	.024	-.073	-.174	-.170	-.153	-.146	-.136	-.143	-.131	-.136	-.142	-.142	—	—	—	—	—
16.75	.213	.182	.116	.025	-.074	-.170	-.160	-.154	-.140	-.135	-.145	-.137	-.132	-.136	-.138	-.119	-.140	-.072	.030	.115
17.41	.217	.194	.120	.023	-.073	-.164	-.160	-.137	-.133	-.143	-.154	-.138	-.155	-.150	-.150	-.135	-.163	-.076	.029	.114
18.08	.220	.194	.116	.020	-.073	-.160	-.153	-.131	-.130	-.136	-.151	-.135	-.141	-.144	-.142	—	—	—	—	—
18.75	—	—	—	—	—	-.154	-.149	-.131	-.127	-.138	-.153	-.136	-.136	-.139	-.138	-.143	-.163	-.070	.038	.129
19.41	.202	.181	.060	.018	-.076	-.144	-.143	-.129	-.127	-.125	-.148	-.134	-.136	-.135	-.138	-.147	-.164	-.072	.033	.126
20.08	.200	.179	.109	.017	-.073	-.134	-.131	-.119	-.133	-.136	-.144	-.142	-.136	-.130	-.132	—	—	—	—	—
20.75	.201	.182	.114	.022	-.070	-.130	-.114	-.123	-.135	-.135	-.146	-.149	-.133	-.125	-.128	-.157	-.163	-.076	.027	.110

(f) $\alpha = 24.5^{\circ}$

$\frac{x}{d}$	Radial angle, θ																			
	0°	15°	30°	45°	60°	90°	105°	120°	135°	150°	180°	195°	210°	225°	240°	270°	285°	300°	315°	330°
6.08	0.264	0.250	0.179	0.064	-0.030	-0.205	-0.184	-0.194	-0.196	-0.210	-0.130	-0.196	-0.197	-0.188	-0.181	-0.208	-0.120	-0.016	0.093	0.188
6.74	.273	.241	.172	.077	-.057	-.187	-.177	-.185	-.193	-.202	-.132	-.185	-.190	-.154	-.177	-.207	-.136	-.057	.073	.173
7.41	.262	.232	.164	.069	-.040	-.178	-.169	-.170	-.185	-.193	-.127	-.190	-.183	-.172	-.160	-.190	-.144	-.045	.062	.158
8.08	.254	.224	.158	.062	-.048	-.167	-.166	-.168	-.179	-.182	-.123	-.184	-.180	-.166	-.158	-.177	-.148	-.050	.055	.152
8.75	.247	.228	.152	.036	-.050	-.163	-.150	-.154	-.176	-.173	-.123	-.178	-.176	-.160	-.152	-.172	-.150	-.050	.054	.154
9.41	.241	.214	.145	.036	-.053	-.162	-.162	-.162	-.166	-.168	-.125	-.174	-.170	-.164	-.150	-.167	-.154	-.060	.045	.143
10.08	.241	.216	.151	.038	-.052	-.163	-.165	-.159	-.162	-.168	-.126	-.166	-.166	-.153	-.152	-.163	-.156	-.065	.044	.141
10.75	.240	.216	.152	.038	-.053	-.160	-.147	-.154	-.156	-.162	-.129	-.161	-.166	-.158	-.152	-.158	-.162	-.066	.041	.141
11.41	.234	.209	.143	.049	-.050	-.164	-.161	-.155	-.149	-.160	-.139	-.162	-.163	-.154	-.137	-.152	-.160	-.064	.040	.138
12.08	.233	.213	.147	.052	-.049	-.175	-.170	-.155	-.156	-.165	-.145	-.158	-.160	-.156	-.133	—	—	—	—	—
12.75	.234	.212	.148	.038	-.049	-.163	-.163	-.150	-.157	-.165	-.130	-.149	-.154	-.140	-.128	-.135	-.155	-.069	.037	.129
13.41	.233	.219	.150	.038	-.050	-.163	-.151	-.137	-.135	-.140	-.143	-.143	-.163	-.158	-.164	-.154	-.157	-.061	.031	.120
14.08	.241	.214	.145	.047	-.052	-.160	-.153	-.137	-.130	-.131	-.143	-.141	-.159	-.158	-.167	-.154	-.157	-.062	.039	.131
14.75	.233	.208	.141	.046	-.054	-.160	-.154	-.137	-.128	-.132	-.144	-.138	-.155	-.156	-.168	-.154	-.154	-.063	.048	.141
15.41	.235	.206	.141	.045	-.053	-.159	-.153	-.134	-.125	-.133	-.145	-.139	-.155	-.159	-.170	-.156	-.156	-.068	.040	.131
16.08	.226	.210	.144	.047	-.052	-.159	-.157	-.135	-.130	-.130	-.146	-.138	-.155	-.157	-.167	-.158	-.158	-.070	.039	.128
16.75	.236	.209	.145	.049	-.052	-.154	-.134	-.133	-.132	-.132	-.147	-.140	-.153	-.154	-.160	-.163	-.160	-.076	.037	.130
17.41	.247	.222	.152	.052	-.052	-.151	-.142	-.142	-.151	-.152	-.150	-.155	-.158	-.148	-.145	-.167	-.161	-.060	.031	.126
18.08	.241	.216	.147	.047	-.056	-.143	-.133	-.153	-.156	-.159	-.155	-.158	-.147	-.143	-.137	-.180	-.160	-.062	.040	.125
18.75	.239	.213	.144	.044	-.056	-.135	-.137	-.159	-.169	-.163	-.165	-.161	-.143	-.135	-.134	-.195	-.161	-.061	.046	.139
19.41	.233	.209	.141	.043	-.055	-.139	-.125	-.160	-.175	-.172	-.171	-.168	-.146	-.145	-.137	-.205	-.167	-.067	.039	.130
20.08	.234	.211	.143	.045	-.053	-.136	-.149	-.169	-.181	-.179	-.179	-.173	-.146	-.143	-.140	-.210	-.174	-.072	.035	.126
20.75	.233	.211	.146	.047	-.054	-.163	-.133	-.166	-.179	-.179	-.188	-.177	-.149	-.147	-.144	-.220	-.175	-.072	.037	.129

(g) $\alpha = 26.5^{\circ}$

$\frac{x}{d}$	Radial angle, θ																			
	0°	15°	30°	45°	60°	90°	105°	120°	135°	150°	180°	195°	210°	225°	240°	270°	285°	300°	315°	330°
6.08	0.344	0.306	0.229	0.121	-0.008	-0.206	-0.198	-0.202	-0.205	-0.220	-0.164	-0.220	-0.211	-0.199	-0.189	-0.206	-0.110	0.004	0.127	0.233
6.74	.336	.298	.221	.112	-.027	-.199	-.189	-.192	-.198	-.211	-.148	-.217	-.202	-.193	-.185	-.214	-.134	-.013	.111	.227
7.41	.324	.291	.215	.105	.088	-.194	-.183	-.187	-.196	-.204	-.145	-.213	-.201	-.183	-.175	-.218	-.137	-.027	.095	.198
8.08	.312	.281	.203	.095	-.086	-.183	-.178	-.177	-.187	-.191	-.144	-.206	-.196	-.180	-.167	-.197	-.138	-.031	.090	.198
8.75	.300	.272	.198	.090	-.089	-.176	-.177	-.169	-.179	-.183	-.145	-.196	-.183	-.175	-.168	-.181	-.137	-.032	.088	.189
9.41	.294	.266	.193	.089	-.031	-.172	-.177	-.167	-.171	-.178	-.150	-.187	-.183	-.173	-.165	-.168	-.143	-.042	.076	.184
10.08	.290	.263	.191	.090	-.085	-.171	-.169	-.158	-.159	-.168	-.154	-.177	-.177	-.169	-.166	-.162	-.138	-.046	.089	.177
10.75	.288	.262	.192	.089	-.082	-.175	-.176	-.158	-.152	-.158	-.160	-.170	-.177	-.175	-.170	-.145	-.138	-.048	.088	.177
11.41	.287	.260	.188	.083	-.086	-.210	-.183	-.173	-.176	-.166	-.174	-.165	-.164	-.153	-.139	-.155	-.147	-.043	.072	.171
12.08	.283	.258	.187	.086	-.084	-.206	-.184	-.172	-.177	-.166	-.178	-.159	-.157	-.139	-.133	—	—	—	—	—
12.75	.282	.256	.189	.086	-.086	-.186	-.192	-.176	-.179	-.164	-.180	-.172	-.149	-.140	-.132	-.151	-.148	-.048	.083	.165
13.41	.321	.262	.202	.085	-.087	-.203	-.193	-.175	-.152	-.152	-.185	-.161	-.172	-.187	-.158	-.153	-.151	-.039	.088	.157
14.08	.307	.274	.193	.083	-.088	-.190	-.189	-.180	-.151	-.153	-.187	-.165	-.167	-.180	-.154	-.168	-.149	-.037	.087	.173
14.75	.300	.268	.190	.084	-.089	-.175	-.177	-.154	-.159	-.162	-.187	-.173	-.166	-.176	-.156	-.171	-.145	-.037	.086	.190
15.41	.293	.261	.187	.082	-.089	-.163	-.188	-.153	-.167	-.178	-.185	-.179	-.165	-.169	-.164	-.187	-.150	-.044	.073	.174
16.08	.287	.258	.189	.082	-.086	-.155	-.159	-.149	-.174	-.191	-.183	-.187	-.162	-.155	-.155	-.196	-.152	-.049	.070	.167
16.75	.285	.257	.187	.083	-.089	-.154	-.147	-.149	-.181	-.191	-.184	-.193	-.160	-.154	-.158	-.216	-.154	-.051	.089	.157
17.41	.317	.264	.203	.090	-.086	-.208	-.171	-.158	-.193	-.195	-.220	-.201	-.170	-.167	-.158	-.215	-.151	-.053	.088	.168
18.08	.306	.258	.198	.084	-.087	-.221	-.164	-.155	-.187	-.196	-.221	-.200	-.169	-.171	-.162	-.219	-.150	-.039	.087	.177
18.75	—	—	—	—	—	-.220	-.193	-.179	-.183	-.175	-.219	-.198	-.177	-.182	-.170	-.209	-.145	-.036	.086	.159
19.41	.292	.265	.189	.080	-.089	-.203	-.203	-.171	-.179	-.175	-.217	-.195	-.163	-.195	-.175	-.198	-.149	-.044	.074	.173
20.08	.286	.261	.187	.080	-.083	-.203	-.212	-.166	-.170	-.170	-.218	-.190	-.187	-.195	-.179	—	—	—	—	—
20.75	.283	.258	.187	.081	-.088	-.221	-.216	-.165	-.169	-.166	-.219	-.191	-.189	-.201	-.184	-.211	-.156	-.053	.067	.167

(h) $\alpha = 29.5^{\circ}$

$\frac{x}{d}$	Radial angle, θ																			
	0°	15°	30°	45°	60°	90°	105°	120°	135°	150°	180°	195°	210°	225°	240°	270°	285°	300°	315°	330°
6.08	0.420	0.364	0.233	0.164	0.018	-0.206	-0.216	-0.221	-0.225	-0.234	-0.199	-0.250	-0.236	-0.229	-0.231	-0.208	-0.108	0.021	0.163	0.294
6.74	.408	.371	.232	.156	.012	-.212	-.225	-.215	-.220	-.223	-.198	-.246	-.227	-.220	-.213	-.218	-.116	.013	.159	.285
7.41	.402	.366	.274	.146	.008	-.217	-.214	-.220	-.225	-.224	-.202	-.227	-.226	-.215	-.209	-.224	-.125	-.004	.133	.264
8.08	.389	.374	.252	.133	-.006	-.220	-.220	-.207	-.205	-.210	-.214	-.221	-.218	-.209	-.211	-.214	-.130	-.008	.131	.258
8.75	.384	.352	.251	.137	-.006	-.221	-.229	-.212	-.203	-.208	-.221	-.211	-.211	-.214	-.208	-.196	-.131	-.008	.131	.254
9.41	.380	.348	.238	.136	-.006	-.220	-.236	-.212	-.194	-.199	-.223	-.201	-.200	-.207	-.208	-.182	-.138	-.017	.123	.250
10.08	.373	.344	.236	.135	-.007	-.220	-.242	-.216	-.198	-.191	-.223	-.198	-.194	-.210	-.207	-.183	-.141	-.025	.115	.238
10.75	.368	.337	.236	.133	-.004	-.216	-.230	-.209	-.189	-.188	-.227	-.221	-.193	-.204	-.204	-.183	-.142	-.024	.108	.233
11.41	.372	.341	.231	.132	.004	-.217	-.217	-.214	-.217	-.213	-.231	-.220	-.216	-.225	-.227	-.227	-.137	-.018	.119	.230
12.08	.365	.336	.233	.133	.004	-.216	-.196	-.197	-.201	-.203	-.235	-.243	-.243	-.221	-.239	—	—	—	—	—
12.75	.377	.330	.233	.130	.004	-.206	-.191	-.197	-.190	-.195	-.238	-.246	-.232	-.234	-.237	-.233	-.140	-.023	.106	.224
13.41	.373	.357	.231	.135	.003	-.215	-.206	-.202	-.207	-.204	-.232	-.244	-.232	-.218	-.220	-.236	-.136	-.015	.130	.226
14.08	.368	.349	.233	.129	-.001	-.216	-.230	-.204	-.209	-.202	-.236	-.240	-.226	-.210	-.211	-.234	-.137	-.013	.130	.232
14.75	.364	.346	.226	.129	-.002	-.219	-.233	-.218	-.211	-.206	-.233	-.232	-.222	-.216	-.209	-.231	-.136	-.012	.131	.232
15.41	.363	.345	.226	.130	.002	-.217	-.238	-.224	-.212	-.209	-.233	-.226	-.219	-.206	-.203	-.227	-.140	-.019	.130	.229
16.08	.358	.342	.233	.132	.004	-.224	-.235	-.230	-.213	-.210	-.232	-.228	-.209	-.207	-.202	-.230	-.142	-.023	.129	.229
16.75	.368	.354	.233	.129	.004	-.220	-.230	-.223	-.210	-.206	-.232	-.225	-.220	-.208	-.201	-.233	-.140	-.026	.112	.222
17.41	.382	.350	.228	.135	.004	-.219	-.232	-.221	-.219	-.214	-.219	-.225	-.223	-.228	-.215	-.233	-.137	-.012	.111	.222
18.08	.368	.351	.219	.127	.002	-.217	-.235	-.223	-.216	-.211	-.219	-.221	-.227	-.225	-.217	—	—	—	—	—
18.75	—	—	—	—	—	-.219	-.235	-.216	-.217	-.213	-.219	-.220	-.229	-.230	-.217	-.235	-.133	-.020	.132	.233
19.41	.378	.349	.239	.131	.003	-.223	-.230	-.217	-.217	-.214	-.218	-.221	-.223	-.220	-.213	-.234	-.139	-.017	.125	.227
20.08	.370	.346	.237	.132	.002	-.223	-.220	-.217	-.219	-.211	-.216	-.222	-.217	-.217	-.211	—	—	—	—	—
20.75	.363	.336	.231	.129	.006	-.219	-.222	-.218	-.217	-.209	-.215	-.222	-.216	-.216	-.209	-.234	-.137	-.025	.113	.229

TABLE I.- EXPERIMENTAL PRESSURE COEFFICIENTS FOR A 33-1/3-CALIBER OGIVE-CYLINDER MODEL AT VARIOUS ANGLES OF ATTACK. $M_o = 1.98$, $Re_o = 0.5 \times 10^6$/INCH, MODEL 1 - Concluded

(i) $\alpha = 32.5^\circ$

$\frac{x}{d}$	Radial angle, θ																			
	0°	15°	30°	45°	60°	90°	105°	120°	135°	150°	180°	195°	210°	225°	240°	270°	285°	300°	315°	330°
6.08	0.506	0.464	0.364	0.212	0.046	-0.196	-0.235	-0.224	-0.239	-0.243	-0.239	-0.255	-0.252	-0.239	-0.232	-0.195	-0.079	0.063	0.224	0.369
6.74	.498	.459	.362	.213	.044	-.201	-.213	-.211	-.212	-.243	-.241	-.265	-.253	-.225	-.216	-.204	-.095	.045	.208	.356
7.41	.507	.462	.358	.205	.040	-.205	-.197	-.207	-.255	-.243	-.242	-.272	-.252	-.214	-.207	-.214	-.100	.038	.200	.340
8.08	.490	.452	.351	.203	.036	-.205	-.196	-.202	-.253	-.242	-.240	-.268	-.249	-.213	-.204	-.213	-.103	.035	.196	.339
8.75	.484	.447	.347	.200	.034	-.206	-.218	-.216	-.241	-.234	-.247	-.261	-.241	-.225	-.212	-.211	-.102	.036	.193	.344
9.41	.479	.442	.343	.197	.035	-.203	-.253	-.235	-.221	-.223	-.245	-.243	-.225	-.240	-.226	-.211	-.104	.028	.185	.332
10.08	.460	.432	.335	.196	.036	-.203	-.274	-.256	-.211	-.211	-.236	-.224	-.213	-.253	-.240	-.210	-.105	.023	.182	.324
10.75	.464	.430	.337	.196	.037	-.199	-.265	-.251	-.208	-.205	-.235	-.227	-.215	-.252	-.244	-.211	-.111	.024	.175	.320
11.41	.473	.437	.334	---	.045	-.207	-.244	-.235	---	-.241	-.241	-.241	-.236	---	-.230	-.216	-.105	.027	---	.317
12.08	.461	.429	.329	---	.046	-.206	-.225	-.220	---	-.224	-.237	-.245	-.248	---	-.249	---	---	---	---	---
12.75	.458	.425	.322	---	.047	-.203	-.215	-.210	---	-.215	-.232	-.243	-.250	---	-.256	-.216	-.112	.023	---	.306
13.41	.515	.459	.349	.199	.048	-.213	-.237	-.235	-.244	-.249	-.241	-.250	-.241	-.235	-.234	-.220	-.110	.033	.202	.307
14.08	.496	.449	.347	.199	.049	-.210	-.254	-.239	-.231	-.237	-.237	-.242	-.235	-.241	-.240	-.219	-.108	-.033	.201	.332
14.75	.492	.444	.344	.196	.049	-.210	-.263	-.241	-.226	-.229	-.235	-.233	-.229	-.243	-.246	-.214	-.106	.034	.200	.340
15.41	.487	.441	.339	.195	.049	-.205	-.258	-.235	-.222	-.225	-.233	-.230	-.225	-.237	-.241	-.215	-.108	.031	.192	.326
16.08	.475	.431	.333	.194	.050	-.205	-.241	-.225	-.225	-.225	-.228	-.231	-.225	-.228	-.230	-.215	-.110	.028	.187	.319
16.75	.471	.428	.337	.195	.051	-.201	-.223	-.217	-.225	-.225	-.226	-.234	-.228	-.223	-.222	-.215	-.111	.023	.181	.313
17.41	.503	.465	.354	.201	.052	-.211	-.243	-.234	-.233	-.235	-.236	-.239	-.229	-.237	-.233	-.219	-.105	.037	.204	.325
18.08	.493	.456	.351	.201	.052	-.208	-.248	-.231	-.234	-.229	-.235	-.236	-.231	-.231	-.235	-.220	-.104	.036	.204	.328
18.75	.488	.449	.348	.199	.051	-.207	-.247	-.231	-.234	-.229	-.235	-.237	-.230	-.229	-.235	-.213	-.099	.037	.201	.341
19.41	.480	.446	.343	.197	.053	-.203	-.243	-.229	-.229	-.230	-.235	-.235	-.228	-.230	-.228	-.214	-.103	.033	.193	.329
20.08	.469	.436	.337	.196	.053	-.203	-.237	-.225	-.226	-.230	-.231	-.233	-.225	-.226	-.226	---	---	---	---	---
20.75	.465	.433	.336	.195	.054	-.200	-.230	-.219	-.221	-.223	-.231	-.233	-.228	-.228	-.225	-.215	-.108	.025	.183	.315

(j) $\alpha = 35.5^\circ$

$\frac{x}{d}$	Radial angle, θ																			
	0°	15°	30°	45°	60°	90°	105°	120°	135°	150°	180°	195°	210°	225°	240°	270°	285°	300°	315°	330°
6.08	0.604	0.567	0.449	0.275	0.088	-0.186	-0.262	-0.219	-0.229	-0.228	-0.268	-0.242	-0.271	-0.278	-0.274	-0.188	-0.056	0.102	0.284	0.447
6.74	.584	.540	.427	.260	.072	-.213	-.231	-.247	-.254	-.226	-.261	-.258	-.250	-.245	-.245	-.189	-.074	.083	.266	.432
7.41	.589	.544	.427	.255	.069	-.197	-.218	-.272	-.280	-.269	-.261	-.267	-.229	-.223	-.213	-.200	-.085	.071	.249	.400
8.08	.577	.531	.418	.250	.064	-.201	-.209	-.286	-.288	-.277	-.254	-.266	-.227	-.226	-.205	-.201	-.084	.087	.215	.409
8.75	.574	.531	.418	.250	.065	-.198	-.230	-.254	-.264	-.267	-.258	-.267	-.248	-.250	-.222	-.200	-.082	.074	.254	.422
9.41	.576	.536	.421	.256	.071	-.196	-.267	-.232	-.239	-.248	-.254	-.252	-.265	-.270	-.252	-.203	-.085	.068	.246	.412
10.08	.571	.533	.422	.258	.074	-.197	-.268	-.220	-.230	-.231	-.248	-.240	-.266	-.275	-.274	-.203	-.088	.062	.242	.405
10.75	.566	.529	.422	.260	.075	-.191	-.260	-.222	-.230	-.224	-.242	-.240	-.259	-.259	-.264	-.206	-.091	.059	.237	.400
11.41	.571	.530	.412	.252	.082	-.193	-.266	-.262	-.259	-.255	-.245	-.246	-.246	-.240	-.243	-.198	-.083	.069	.244	.398
12.08	.566	.527	.414	.255	.087	-.192	-.266	-.268	-.268	-.260	-.241	-.238	-.236	-.229	-.239	---	---	---	---	---
12.75	.560	.523	.415	.258	.089	-.187	-.250	-.246	-.249	-.247	-.237	-.237	-.237	-.233	-.230	-.201	-.088	.059	.233	.387
13.41	.594	.536	.417	.251	.084	-.201	-.236	-.250	-.227	-.254	-.243	-.248	-.229	-.250	-.224	-.206	-.086	.064	.250	.365
14.08	.584	.532	.412	.246	.080	-.202	-.255	-.237	-.233	-.245	-.242	-.240	-.238	-.248	-.234	-.204	-.084	.069	.250	.396
14.75	.585	.530	.414	.249	.081	-.201	-.264	-.225	-.240	-.232	-.241	-.235	-.247	-.238	-.246	-.203	-.082	.072	.259	.416
15.41	.588	.532	.418	.254	.088	-.198	-.258	-.225	-.246	-.229	-.239	-.236	-.244	-.230	-.249	-.205	-.085	.067	.254	.408
16.08	.582	.534	.420	.257	.091	-.198	-.240	-.233	-.244	-.234	-.238	-.240	-.238	-.231	-.240	-.206	-.088	.063	.250	.401
16.75	.575	.528	.422	.257	.092	-.193	-.225	-.235	-.231	-.234	-.236	-.240	-.230	-.234	-.229	-.207	-.090	.061	.243	.396
17.41	.554	.512	.399	.235	.088	-.202	-.225	-.231	-.230	-.225	-.236	-.232	-.235	-.233	-.221	-.208	-.084	.060	.234	.389
18.08	.560	.517	.403	.236	.089	-.201	-.231	-.239	-.233	-.226	-.242	-.233	-.235	-.240	-.225	-.208	-.083	.064	.240	.399
18.75	.556	.515	.401	.237	.087	-.201	-.231	-.239	-.237	-.226	-.240	-.234	-.235	-.237	-.225	-.204	-.083	.067	.245	.418
19.41	.552	.511	.398	.237	.093	-.197	-.238	-.239	-.237	-.226	-.241	-.231	-.238	-.235	-.226	-.208	-.091	.059	.233	.411
20.08	.545	.507	.397	.237	.095	-.201	-.238	-.237	-.240	-.226	-.240	-.231	-.239	-.233	-.226	-.212	-.093	.054	.229	.406
20.75	.541	.503	.374	.236	.095	-.196	-.231	-.228	-.233	-.223	-.239	-.229	-.237	-.231	-.223	-.214	-.093	.049	.225	.398

TABLE II.- EXPERIMENTAL PRESSURE COEFFICIENTS FOR A 33-1/3-CALIBER OGIVE-CYLINDER MODEL AT VARIOUS ANGLES OF ATTACK. $M_o = 1.98$, $Re_o = 0.5 \times 10^6$/INCH, MODEL 2

(a) $\alpha = 0^\circ$

$\frac{x}{d}$	Radial angle, θ																		
	0°	15°	30°	45°	60°	75°	90°	105°	120°	135°	150°	165°	180°	195°	210°	225°	240°	255°	270°
0.44	0.081	0.081	0.081	0.080	0.081	0.082	0.082	0.082	0.082	0.082	0.083	0.082	0.082	0.083	0.082	0.081	0.081	0.082	0.082
.89	.072	.073	.073	.073	.074	.075	.075	.075	.074	.075	.075	.074	.074	.075	.075	.074	.074	.075	.075
1.33	.064	.065	.064	.064	.064	.065	.065	.065	.066	.067	.068	.067	.066	.067	.066	.065	.065	.065	.065
1.78	.048	.048	.047	.047	.048	.049	.050	.050	.049	.050	.051	.050	.050	.051	.051	.051	.050	.051	.051
2.22	.035	.035	.035	.036	.037	.038	.038	.036	.036	.037	.037	.036	.035	.036	.036	.035	.035	.036	.037
2.67	.023	.024	.024	.024	.025	.026	.026	.026	.025	.026	.026	.025	.023	.023	.022	.022	.022	.023	.023
3.11	.018	.019	.019	.019	.018	.019	.020	.020	.020	.022	.022	.020	.019	.020	.018	.018	.017	.017	.017
3.56	.008	.009	.009	.009	.010	.012	.013	.013	.012	.013	.012	.011	.011	.012	.010	.010	.009	.009	.009
4.00	-.003	-.002	-.002	-.001	-.001	0	0	.001	.001	.002	.001	0	-.002	-.001	-.002	-.002	-.003	-.004	-.004
4.44	-.011	-.010	-.010	-.010	-.010	-.010	-.010	-.010	-.010	-.009	-.010	-.011	-.012	-.011	-.013	-.012	-.014	-.014	-.014
4.89	-.017	-.016	-.016	-.016	-.017	-.016	-.015	-.016	-.017	-.016	-.015	-.017	-.018	-.017	-.019	-.020	-.021	-.021	-.020
5.33	-.026	-.024	-.023	-.020	-.018	-.017	-.017	-.018	-.019	-.020	-.022	-.024	-.025	-.025	-.027	-.027	-.029	-.028	-.027
5.78	-.029	-.027	-.026	-.026	-.027	-.027	-.026	-.026	-.025	-.022	-.022	-.024	-.027	-.027	-.028	-.027	-.027	-.026	-.027
6.22	-.027	-.027	-.028	-.025	-.024	-.022	-.022	-.022	-.022	-.023	-.025	-.026	-.026	-.025	-.026	-.028	-.029	-.027	-.026
6.67	-.024	-.022	-.022	-.022	-.022	-.021	-.020	-.020	-.020	-.020	-.020	-.022	-.023	-.023	-.021	-.019	-.020	-.020	-.019
7.11	-.019	-.019	-.019	-.018	-.018	-.016	-.016	-.016	-.017	-.017	-.018	-.019	-.018	-.017	-.017	-.016	-.017	-.016	-.016
7.55	-.016	-.015	-.015	-.015	-.016	-.015	-.014	-.015	-.015	-.014	-.014	-.014	-.013	-.012	-.013	-.012	-.010	-.009	-.008
8.00	-.013	-.013	-.014	-.014	-.015	-.014	-.013	-.013	-.014	-.013	-.012	-.013	-.013	-.011	-.010	-.009	-.011	-.010	-.009
8.44	-.005	-.006	-.008	-.009	-.012	-.013	-.013	-.013	-.013	-.012	-.012	-.012	-.010	-.008	-.008	-.007	-.009	-.009	-.010
8.89	-.003	-.002	-.004	-.006	-.009	-.011	-.012	-.012	-.013	-.012	-.011	-.010	-.008	-.006	-.006	-.006	-.008	-.009	-.009
9.33	.003	.004	.005	.004	.003	0	-.002	-.004	-.004	-.002	0	.001	.002	.003	.001	.001	.002	.001	.002
9.78	.002	.003	.001	.001	.001	.002	.002	.002	.002	.004	.005	.002	.001	.001	.002	.003	.004	.005	.006
10.22	.008	.007	.005	.004	.004	.004	.005	.006	.005	.006	.005	.004	.006	.007	.005	.005	.006	.008	.009
10.67	.002	.003	.001	0	-.002	-.002	-.002	-.003	-.003	-.001	0	0	0	.002	.002	.002	0	.001	.002
11.33	-.002	-.002	-.003	-.003	-.003	-.004	-.005	-.006	-.006	-.004	-.003	-.002	-.002	-.001	-.001	0	0	.001	.002
12.00	.001	.001	-.001	-.002	-.002	-.002	-.002	-.003	-.004	-.003	-.002	-.002	0	.002	.003	.003	.003	.003	.005
12.67	-.004	-.004	-.006	-.007	-.008	-.008	-.008	-.009	-.010	-.008	-.007	-.007	-.006	-.004	-.004	-.002	-.002	0	.003
13.33	-.004	-.005	-.006	-.006	-.007	-.006	-.005	-.006	-.006	-.004	-.003	-.005	-.004	-.003	-.002	-.001	-.002	-.001	.001
14.00	-.001	-.001	-.002	-.002	-.002	-.001	.001	.001	.002	.003	.002	.001	.001	.002	.002	.003	.004	.004	.005

(b) $\alpha = 0.9^\circ$

$\frac{x}{d}$	Radial angle, θ																		
	0°	15°	30°	45°	60°	75°	90°	105°	120°	135°	150°	165°	180°	195°	210°	225°	240°	255°	270°
0.44	0.087	0.088	0.087	0.086	0.083	0.081	0.080	0.078	0.077	0.075	0.073	0.073	0.072	0.074	0.074	0.074	0.075	0.076	0.079
.89	.081	.082	.081	.079	.077	.074	.072	.071	.070	.068	.067	.066	.065	.068	.068	.069	.070	.071	.073
1.33	.074	.074	.073	.071	.068	.065	.063	.061	.060	.059	.058	.058	.058	.060	.060	.061	.062	.062	.066
1.78	.058	.058	.058	.055	.043	.050	.048	.046	.046	.045	.044	.044	.043	.044	.043	.044	.044	.045	.048
2.22	.041	.042	.042	.041	.040	.039	.037	.036	.035	.032	.029	.028	.027	.029	.029	.030	.031	.032	.035
2.67	.028	.030	.030	.029	.027	.025	.024	.022	.021	.020	.018	.017	.016	.016	.016	.017	.017	.018	.121
3.11	.023	.024	.024	.023	.021	.019	.018	.016	.016	.015	.014	.010	.013	.014	.013	.012	.013	.013	.015
3.56	.014	.014	.015	.014	.012	.011	.010	.009	.009	.007	.006	.006	.005	.006	.005	.005	.005	.005	.007
4.00	.001	.003	.003	.003	.001	0	-.001	-.002	-.003	-.004	-.005	-.006	-.007	-.006	-.006	-.006	-.006	-.006	-.005
4.44	-.010	-.008	-.008	-.009	-.009	-.010	-.011	-.013	-.013	-.015	-.016	-.016	-.017	-.015	-.016	-.016	-.016	-.017	-.015
4.89	-.017	-.015	-.015	-.015	-.016	-.017	-.018	-.018	-.018	-.019	-.021	-.021	-.023	-.021	-.022	-.021	-.022	-.022	-.021
5.33	-.023	-.021	-.021	-.020	-.020	-.019	-.020	-.019	-.019	-.022	-.026	-.027	-.028	-.027	-.027	-.028	-.029	-.029	-.028
5.78	-.026	-.023	-.021	-.023	-.024	-.025	-.026	-.026	-.025	-.024	-.025	-.027	-.029	-.028	-.029	-.029	-.029	-.025	-.023
6.22	-.025	-.025	-.025	-.024	-.021	-.019	-.019	-.019	-.020	-.027	-.029	-.028	-.028	-.026	-.026	-.027	-.031	-.031	-.028
6.67	-.025	-.022	-.021	-.022	-.021	-.019	-.018	-.019	-.018	-.019	-.019	-.022	-.025	-.022	-.022	-.019	-.018	-.018	-.016
7.11	-.020	-.019	-.018	-.019	-.017	-.016	-.017	-.017	-.017	-.017	-.017	-.018	-.019	-.017	-.016	-.014	-.014	-.016	-.016
7.55	-.015	-.014	-.014	-.014	-.013	-.014	-.015	-.015	-.015	-.015	-.014	-.012	-.014	-.014	-.013	-.010	-.009	-.008	-.006
8.00	-.014	-.013	-.013	-.014	-.013	-.013	-.014	-.014	-.014	-.014	-.013	-.011	-.010	-.008	-.006	-.015	-.007	-.008	-.008
8.44	-.012	-.012	-.013	-.011	-.011	-.012	-.013	-.013	-.011	-.011	-.009	-.007	-.004	-.001	-.003	-.003	-.004	-.005	-.005
8.89	-.010	-.010	-.011	-.011	-.012	-.013	-.012	-.012	-.010	-.009	-.008	-.007	-.006	-.002	-.004	-.005	-.006	-.008	-.008
9.33	.001	.001	.001	0	-.002	-.003	-.003	-.003	-.001	-.001	-.002	0	.001	.003	.002	0	-.001	-.001	0
9.78	.002	.003	.005	.002	-.001	-.002	-.004	-.004	-.003	-.002	-.001	0	-.001	.001	.002	.003	.002	.001	.001
10.22	.009	.010	.008	.004	.001	0	-.001	-.002	-.001	-.001	0	.001	.003	.007	.006	.005	.004	.003	.004
10.67	.003	.003	.002	-.002	-.005	-.006	-.007	-.007	-.006	-.005	-.004	-.002	-.001	.002	.002	.001	-.001	-.003	-.002
11.33	.002	.002	0	-.003	-.006	-.008	-.009	-.009	-.007	-.006	-.005	-.004	-.004	-.002	-.002	-.001	-.002	-.003	-.002
12.00	.005	.004	.002	0	-.004	-.006	-.008	-.009	-.008	-.006	-.005	-.003	-.001	.002	.002	.002	0	-.001	.001
12.67	-.004	-.003	-.004	-.007	-.009	-.011	-.012	-.012	-.010	-.008	-.005	-.004	-.005	-.003	-.003	-.004	-.005	-.006	-.004
13.33	-.003	-.005	-.005	-.007	-.007	-.007	-.007	-.006	-.005	-.005	-.005	-.004	-.004	-.002	-.002	-.002	-.003	-.003	-.002
14.00	0	.001	.001	.001	0	.001	0	0	0	0	0	.001	0.	.001	0	0	-.001	0	.002

NACA

TABLE II.- EXPERIMENTAL PRESSURE COEFFICIENTS FOR A 33-1/3-CALIBER OGIVE-CYLINDER MODEL AT VARIOUS ANGLES OF ATTACK. $M_o = 1.98$, $Re_o = 0.5 \times 10^6$/INCH, MODEL 2 - Continued

(c) $\alpha = 2.0^\circ$

$\frac{x}{d}$	Radial angle, θ																		
	0°	15°	30°	45°	60°	75°	90°	105°	120°	135°	150°	165°	180°	195°	210°	225°	240°	255°	270°
0.44	0.103	0.102	0.099	0.095	0.091	0.086	0.081	0.076	0.073	0.070	0.068	0.067	0.067	0.067	0.068	0.070	0.073	0.077	0.081
.89	.094	.093	.090	.086	.084	.079	.074	.069	.066	.063	.061	.060	.060	.059	.060	.062	.065	.069	.072
1.33	.084	.083	.080	.076	.073	.068	.064	.060	.057	.054	.053	.052	.052	.052	.053	.054	.057	.060	.063
1.78	.066	.065	.062	.058	.055	.051	.047	.043	.042	.039	.038	.038	.039	.037	.038	.039	.041	.043	.045
2.22	.052	.050	.048	.044	.042	.039	.035	.031	.028	.025	.023	.022	.023	.022	.022	.024	.026	.029	.031
2.67	.038	.038	.037	.034	.031	.027	.022	.019	.017	.014	.012	.012	.011	.010	.010	.010	.012	.015	.018
3.11	.033	.032	.030	.027	.025	.021	.017	.014	.013	.011	.010	.008	.008	.007	.008	.008	.010	.010	.012
3.56	.022	.021	.019	.017	.016	.013	.009	.006	.006	.004	.003	.001	0	0	0	0	.001	.002	.004
4.00	.008	.007	.005	.004	.004	.001	-.002	-.005	-.006	-.008	-.008	-.009	-.011	-.011	-.011	-.011	-.009	-.008	-.006
4.44	-.005	-.005	-.007	-.008	-.009	-.011	-.014	-.016	-.017	-.019	-.021	-.021	-.020	-.020	-.021	-.022	-.021	-.020	-.018
4.89	-.011	-.012	-.014	-.013	-.014	-.017	-.020	-.022	-.022	-.024	-.025	-.024	-.022	-.024	-.025	-.026	-.024	-.024	-.024
5.33	-.020	-.020	-.021	-.018	-.016	-.019	-.021	-.023	-.023	-.026	-.030	-.030	-.029	-.029	-.030	-.031	-.030	-.031	-.031
5.78	-.024	-.022	-.020	-.019	-.021	-.024	-.027	-.029	-.027	-.027	-.028	-.027	-.027	-.030	-.031	-.032	-.032	-.033	-.032
6.22	-.022	-.023	-.024	-.026	-.021	-.020	-.022	-.023	-.023	-.029	-.029	-.027	-.026	-.027	-.029	-.028	-.028	-.031	-.032
6.67	-.020	-.019	-.014	-.016	-.017	-.019	-.021	-.022	-.021	-.021	-.021	-.021	-.021	-.020	-.019	-.021	-.021	-.022	-.022
7.11	-.017	-.017	-.016	-.017	-.016	-.018	-.020	-.021	-.020	-.020	-.019	-.016	-.014	-.015	-.016	-.016	-.016	-.017	-.019
7.55	-.012	-.013	-.013	-.014	-.014	-.018	-.020	-.021	-.019	-.017	-.014	-.012	-.009	-.009	-.010	-.012	-.010	-.010	-.010
8.00	-.011	-.011	-.013	-.014	-.016	-.018	-.019	-.019	-.017	-.015	-.013	-.010	-.008	-.007	-.006	-.007	-.009	-.010	-.011
8.44	-.006	-.009	-.011	-.013	-.014	-.015	-.016	-.016	-.013	-.010	-.008	-.005	-.002	-.003	-.003	-.005	-.006	-.008	-.009
8.89	-.005	-.007	-.012	-.014	-.013	-.014	-.014	-.014	-.011	-.010	-.007	-.007	-.005	-.006	-.006	-.007	-.007	-.008	-.010
9.33	.002	.001	-.004	-.005	-.003	-.004	-.005	-.006	-.004	-.004	-.004	-.003	-.002	-.003	-.004	-.005	-.004	-.005	-.004
9.78	-.001	-.001	-.003	-.005	-.005	-.006	-.006	-.007	-.005	-.005	-.004	-.004	-.003	-.004	-.004	-.003	0	0	-.001
10.22	.006	.003	0	-.003	-.003	-.005	-.006	-.006	-.005	-.004	-.004	-.002	-.001	.001	.001	0	.001	-.001	-.001
10.67	.004	.002	-.002	-.006	-.008	-.010	-.011	-.011	-.009	-.009	-.007	-.006	-.004	-.003	-.003	-.003	-.003	-.005	-.005
11.33	.003	0	-.003	-.006	-.008	-.011	-.012	-.012	-.010	-.009	-.007	-.006	-.004	-.004	-.003	-.004	-.002	-.003	-.003
12.00	.008	.004	0	-.005	-.007	-.010	-.010	-.009	-.006	-.005	-.004	-.002	0	0	-.001	-.002	-.001	-.002	-.002
12.67	.002	0	-.004	-.008	-.010	-.013	-.014	-.013	-.010	-.008	-.006	-.004	-.003	-.003	-.004	-.006	-.006	-.007	-.008
13.33	-.002	-.004	-.006	-.007	-.006	-.008	-.009	-.009	-.006	-.005	-.004	-.003	-.002	-.003	-.003	-.005	-.005	-.007	-.007
14.00	.005	.004	.001	-.001	0	-.002	-.003	-.003	-.001	-.001	-.001	0	.001	0	-.002	-.003	-.003	-.004	-.005

(d) $\alpha = 4.0^\circ$

$\frac{x}{d}$	Radial angle, θ																		
	0°	15°	30°	45°	60°	75°	90°	105°	120°	135°	150°	165°	180°	195°	210°	225°	240°	255°	270°
0.44	0.129	0.127	0.119	0.110	0.099	0.087	0.076	0.067	0.059	0.054	0.052	0.050	0.049	0.051	0.051	0.053	0.058	0.064	0.074
.89	.120	.120	.113	.105	.094	.082	.071	.061	.053	.048	.045	.044	.048	.047	.043	.045	.049	.054	.063
1.33	.108	.107	.100	.092	.081	.070	.059	.052	.044	.039	.038	.040	.039	.040	.037	.037	.041	.047	.054
1.78	.086	.085	.078	.070	.060	.050	.040	.033	.027	.024	.024	.022	.022	.022	.024	.024	.026	.030	.037
2.22	.068	.067	.062	.056	.048	.039	.031	.024	.018	.015	.014	.012	.011	.011	.012	.012	.014	.018	.025
2.67	.053	.053	.047	.041	.032	.024	.015	.008	.004	.002	.003	.002	.002	.002	.002	0	.001	.004	.008
3.11	.045	.044	.038	.032	.025	.017	.011	.005	.006	.005	.003	.001	.002	.002	.003	-.003	.001	.001	.005
3.56	.033	.033	.029	.024	.017	.010	.004	0	-.004	-.006	-.006	-.007	-.006	-.007	-.008	-.007	-.007	-.006	-.004
4.00	.023	.022	.017	.011	.004	-.003	-.007	-.012	-.015	-.016	-.015	-.016	-.015	-.015	-.017	-.018	-.018	-.017	-.015
4.44	.010	.009	.006	0.	-.008	-.014	-.019	-.024	-.026	-.026	-.025	-.025	-.024	-.024	-.025	-.027	-.028	-.028	-.025
4.89	.002	.001	-.002	-.009	-.015	-.019	-.024	-.029	-.029	-.029	-.027	-.026	-.025	-.026	-.028	-.030	-.033	-.035	-.032
5.33	-.010	-.010	-.012	-.016	-.018	-.022	-.029	-.033	-.031	-.030	-.029	-.029	-.029	-.C30	-.032	-.035	-.037	-.040	-.038
5.78	-.014	-.012	-.013	-.020	-.019	-.027	-.032	-.033	-.033	-.032	-.030	-.029	-.029	-.029	-.032	-.035	-.038	-.040	-.041
6.22	-.015	-.014	-.016	-.024	-.028	-.029	-.031	-.033	-.031	-.030	-.027	-.025	-.024	-.024	-.027	-.031	-.037	-.042	-.043
6.67	-.014	-.014	-.013	-.019	-.022	-.026	-.028	-.029	-.026	-.022	-.018	-.016	-.015	-.016	-.019	-.019	-.021	-.027	-.030
7.11	-.009	-.009	-.012	-.018	-.022	-.027	-.029	-.028	-.024	-.020	-.016	-.014	-.011	-.009	-.011	-.014	-.019	-.024	-.027
7.55	-.009	-.006	-.010	-.016	-.019	-.024	-.026	-.026	-.023	-.020	-.016	-.013	-.010	-.009	-.012	-.014	-.017	-.020	-.022
8.00	-.006	-.006	-.012	-.019	-.022	-.025	-.026	-.025	-.022	-.019	-.016	-.013	-.010	-.009	-.008	-.009	-.012	-.017	-.020
8.44	-.004	-.005	-.008	-.012	-.017	-.020	-.021	-.020	-.017	-.015	-.012	-.010	-.007	-.007	-.009	-.011	-.012	-.015	-.017
8.89	-.005	-.005	-.010	-.014	-.017	-.020	-.020	-.019	-.016	-.014	-.012	-.011	-.009	-.010	-.011	-.011	-.012	-.015	-.018
9.33	.001	.002	-.002	-.005	-.009	-.013	-.015	-.014	-.011	-.010	-.008	-.007	-.003	-.005	-.007	-.008	-.008	-.011	-.012
9.78	.002	-.001	-.004	-.007	-.011	-.014	-.015	-.014	-.011	-.009	-.007	-.006	-.003	-.003	-.004	-.006	-.007	-.011	-.013
10.22	.007	.004	.001	-.004	-.008	-.011	-.012	-.011	-.009	-.008	-.006	-.004	.001	-.001	-.003	-.004	-.005	-.006	-.007
10.67	.003	-.002	-.006	-.009	-.013	-.015	-.015	-.013	-.011	-.010	-.008	-.008	-.003	-.003	-.004	-.004	-.005	-.008	-.009
11.33	.002	-.001	-.004	-.009	-.013	-.017	-.017	-.015	-.011	-.009	-.007	-.007	-.003	-.003	-.004	-.005	-.006	-.010	-.011
12.00	.013	.008	.002	-.004	-.008	-.011	-.012	-.010	-.008	-.007	-.006	-.005	.001	-.002	-.004	-.005	-.005	-.007	-.007
12.67	.007	.005	-.001	-.007	-.012	-.014	-.013	-.011	-.008	-.007	-.006	-.006	-.002	-.004	-.005	-.006	-.008	-.012	-.013
13.33	.008	.005	-.001	-.007	-.011	-.014	-.014	-.011	-.007	-.005	-.004	-.005	-.001	-.003	-.005	-.007	-.009	-.014	-.016
14.00	.014	.011	.006	.001	-.004	-.007	-.008	-.006	-.003	-.001	0	0	.004	0	-.003	-.005	-.008	-.013	-.015

TABLE II.- EXPERIMENTAL PRESSURE COEFFICIENTS FOR A 33-1/3-CALIBER OGIVE-CYLINDER MODEL AT VARIOUS ANGLES OF ATTACK. $M_o = 1.98$, $Re_o = 0.5 \times 10^6$/INCH, MODEL 2 - Continued

(e) $\alpha = 5.7^\circ$

$\frac{x}{d}$	Radial angle, θ																		
	0°	15°	30°	45°	60°	75°	90°	105°	120°	135°	150°	165°	180°	195°	210°	225°	240°	255°	270°
0.44	0.162	0.157	0.144	0.126	0.103	0.080	0.061	0.046	0.039	0.035	0.034	0.036	0.037	0.036	0.034	0.034	0.038	0.047	0.062
.89	.152	.149	.138	.121	.099	.076	.056	.040	.032	.028	.027	.029	.030	.029	.028	.027	.029	.036	.047
1.33	.137	.132	.120	.102	.081	.059	.041	.028	.022	.019	.019	.022	.023	.025	.022	.021	.023	.030	.042
1.78	.114	.110	.099	.084	.064	.043	.026	.013	.008	.006	.006	.009	.010	.011	.009	.007	.008	.015	.026
2.22	.097	.094	.084	.068	.049	.029	.012	.001	-.004	-.004	-.002	.003	.004	.002	.001	-.002	-.003	.002	.017
2.67	.079	.076	.066	.052	.033	.015	0	-.011	-.012	-.011	-.009	-.005	-.004	-.005	-.007	-.010	-.013	-.010	-.002
3.11	.069	.065	.055	.041	.024	.006	-.006	-.010	-.010	-.010	-.008	-.004	-.003	-.004	-.007	-.011	-.012	-.014	-.009
3.56	.055	.053	.044	.031	.013	-.003	-.013	-.019	-.021	-.018	-.014	-.011	-.010	-.011	-.015	-.019	-.023	-.021	-.017
4.00	.038	.035	.028	.016	.001	-.014	-.023	-.030	-.030	-.026	-.022	-.018	-.017	-.018	-.021	-.025	-.030	-.030	-.026
4.44	.021	.018	.011	0	-.014	-.027	-.034	-.041	-.038	-.033	-.029	-.025	-.023	-.025	-.028	-.033	-.039	-.041	-.038
4.89	.010	.008	.001	-.009	-.020	-.030	-.039	-.043	-.040	-.035	-.030	-.027	-.026	-.027	-.031	-.037	-.044	-.048	-.047
5.33	-.002	-.004	-.010	-.019	-.030	-.037	-.042	-.046	-.043	-.038	-.034	-.030	-.029	-.032	-.036	-.041	-.047	-.053	-.054
5.78	-.007	-.007	-.011	-.021	-.035	-.045	-.050	-.050	-.045	-.038	-.032	-.028	-.027	-.029	-.033	-.038	-.046	-.053	-.057
6.22	-.006	-.008	-.014	-.023	-.035	-.048	-.054	-.054	-.046	-.037	-.030	-.025	-.023	-.005	-.030	-.036	-.045	-.054	-.059
6.67	-.005	-.006	-.013	-.020	-.030	-.040	-.047	-.048	-.040	-.031	-.025	-.022	-.019	-.021	-.026	-.032	-.039	-.046	-.050
7.11	-.007	-.006	-.013	-.022	-.033	-.042	-.048	-.047	-.037	-.029	-.024	-.019	-.015	-.017	-.019	-.022	-.028	-.037	-.042
7.55	-.004	-.007	-.015	-.024	-.035	-.042	-.047	-.043	-.034	-.026	-.022	-.017	-.010	-.011	-.014	-.018	-.024	-.035	-.042
8.00	0	-.001	-.012	-.024	-.036	-.045	-.048	-.043	-.033	-.025	-.021	-.016	-.009	-.013	-.016	-.017	-.020	-.028	-.035
8.44	.001	-.001	-.010	-.021	-.032	-.040	-.042	-.037	-.027	-.022	-.020	-.016	-.008	-.011	-.015	-.017	-.021	-.029	-.036
8.89	.003	-.001	-.009	-.018	-.027	-.036	-.040	-.035	-.025	-.020	-.019	-.016	-.009	-.014	-.017	-.017	-.020	-.027	-.034
9.33	.001	.006	-.005	-.016	-.025	-.029	-.031	-.026	-.018	-.015	-.015	-.010	.001	-.006	-.012	-.012	-.012	-.015	-.022
9.78	.003	.005	-.005	-.016	-.024	-.030	-.031	-.025	-.017	-.015	-.015	-.010	.002	-.004	-.010	-.010	-.012	-.017	-.023
10.22	.007	.010	.001	-.010	-.018	-.023	-.026	-.021	-.015	-.013	-.013	-.007	.005	-.003	-.010	-.011	-.012	-.017	-.023
10.67	.007	.005	-.004	-.016	-.022	-.029	-.028	-.023	-.016	-.014	-.015	-.012	0	-.008	-.013	-.012	-.013	-.016	-.022
11.33	.006	.001	-.005	-.014	-.022	-.029	-.029	-.024	-.017	-.015	-.016	-.014	-.001	-.008	-.010	-.009	-.011	-.016	-.022
12.00	.019	.020	.004	-.009	-.016	-.024	-.025	-.020	-.015	-.015	-.015	-.007	.005	-.005	-.011	-.011	-.012	-.013	-.016
12.67	.010	.005	-.002	-.010	-.021	-.028	-.027	-.021	-.015	-.014	-.016	-.014	-.004	-.013	-.014	-.013	-.015	-.019	-.025
13.33	.016	.010	.002	-.009	-.020	-.028	-.026	-.018	-.012	-.010	-.013	-.014	-.005	-.012	-.012	-.012	-.014	-.020	-.028
14.00	.024	.018	.010	.001	-.015	-.017	-.016	-.011	-.007	-.007	-.009	-.007	.001	-.007	-.010	-.010	-.011	-.015	-.023

(f) $\alpha = 8.0^\circ$

$\frac{x}{d}$	Radial angle, θ																		
	0°	15°	30°	45°	60°	75°	90°	105°	120°	135°	150°	165°	180°	195°	210°	225°	240°	255°	270°
0.44	0.187	0.178	0.160	0.134	0.104	0.071	0.047	0.028	0.020	0.019	0.021	0.026	0.026	0.026	0.022	0.020	0.022	0.032	0.052
.89	.176	.171	.155	.131	.103	.069	.044	.023	.014	.013	.015	.020	.021	.020	.018	.015	.014	.020	.037
1.33	.161	.154	.137	.112	.085	.053	.030	.012	.005	.006	.008	.014	.016	.013	.011	.007	.005	.012	.029
1.78	.136	.130	.114	.090	.064	.033	.012	-.005	-.011	-.010	-.007	.003	.005	0	-.003	-.006	-.008	-.003	.012
2.22	.116	.108	.092	.070	.045	.017	-.003	-.017	-.024	-.018	-.011	-.004	-.002	-.004	-.008	-.018	-.022	-.017	-.004
2.67	.098	.093	.080	.058	.033	.004	-.015	-.029	-.028	-.024	-.018	-.010	-.008	-.010	-.017	-.023	-.031	-.032	-.020
3.11	.093	.087	.071	.048	.023	-.005	-.024	-.032	-.033	-.026	-.020	-.011	-.009	-.012	-.018	-.027	-.034	-.037	-.027
3.56	.073	.073	.059	.037	.013	-.014	-.031	-.040	-.041	-.033	-.024	-.017	-.015	-.018	-.023	-.033	-.043	-.044	-.037
4.00	.058	.053	.040	.020	-.003	-.028	-.044	-.052	-.051	-.042	-.033	-.025	-.023	-.025	-.031	-.040	-.051	-.055	-.047
4.44	.040	.035	.022	.002	-.019	-.043	-.056	-.065	-.061	-.051	-.041	-.033	-.030	-.033	-.038	-.048	-.060	-.067	-.061
4.89	.029	.024	.011	-.008	-.027	-.050	-.063	-.071	-.064	-.051	-.042	-.033	-.030	-.033	-.038	-.048	-.062	-.072	-.069
5.33	.017	.014	0	-.019	-.037	-.055	-.066	-.072	-.062	-.048	-.043	-.037	-.033	-.037	-.042	-.050	-.065	-.078	-.079
5.78	.009	.006	-.003	-.020	-.039	-.062	-.074	-.076	-.063	-.047	-.040	-.033	-.028	-.035	-.040	-.048	-.062	-.079	-.084
6.22	.006	.004	-.010	-.032	-.054	-.074	-.077	-.072	-.057	-.045	-.041	-.033	-.025	-.032	-.035	-.040	-.054	-.076	-.086
6.67	.005	-.002	-.013	-.025	-.046	-.068	-.075	-.069	-.051	-.039	-.035	-.026	-.016	-.025	-.030	-.033	-.043	-.063	-.078
7.11	.003	.004	-.010	-.030	-.050	-.069	-.072	-.063	-.045	-.036	-.032	-.025	-.010	-.020	-.026	-.029	-.036	-.055	-.071
7.55	.007	0	-.013	-.030	-.049	-.067	-.067	-.058	-.041	-.033	-.032	-.023	-.004	-.018	-.024	-.024	-.028	-.043	-.061
8.00	.006	.003	-.010	-.031	-.051	-.066	-.065	-.045	-.035	-.030	-.030	-.024	0	-.014	-.022	-.022	-.026	-.040	-.056
8.44	.004	-.002	-.013	-.032	-.050	-.065	-.061	-.046	-.031	-.028	-.028	-.023	.001	-.017	-.023	-.021	-.024	-.036	-.052
8.89	.003	-.001	-.016	-.034	-.051	-.063	-.057	-.042	-.027	-.025	-.029	-.025	-.002	-.021	-.026	-.020	-.023	-.034	-.051
9.33	.007	.001	-.013	-.028	-.044	-.054	-.047	-.032	-.022	-.021	-.024	-.018	.009	-.015	-.025	-.020	-.022	-.028	-.042
9.78	.009	.004	-.009	-.025	-.038	-.048	-.046	-.032	-.022	-.019	-.024	-.021	.002	-.020	-.020	-.015	-.017	-.025	-.039
10.22	.018	.013	-.001	-.018	-.034	-.044	-.043	-.030	-.022	-.020	-.023	-.021	.007	-.011	-.016	-.014	-.018	-.025	-.039
10.67	.023	.016	0	-.018	-.034	-.048	-.049	-.035	-.024	-.021	-.023	-.025	-.002	-.018	-.017	-.015	-.018	-.028	-.042
11.33	.024	.018	.003	-.016	-.035	-.051	-.050	-.035	-.025	-.021	-.023	-.028	-.009	-.023	-.018	-.015	-.019	-.029	-.044
12.00	.027	.020	.002	-.017	-.035	-.051	-.051	-.037	-.029	-.024	-.024	-.021	-.005	-.017	-.017	-.017	-.022	-.030	-.041
12.67	.020	.013	-.004	-.021	-.038	-.053	-.049	-.032	-.026	-.022	-.022	-.022	-.012	-.022	-.019	-.020	-.023	-.032	-.044
13.33	.017	.010	-.006	-.023	-.039	-.050	-.042	-.026	-.021	-.021	-.021	-.023	-.012	-.019	-.016	-.017	-.018	-.027	-.045
14.00	.023	.016	-.004	-.021	-.033	-.039	-.030	-.018	-.017	-.016	-.017	-.012	-.002	-.013	-.016	-.016	-.018	-.023	-.038

TABLE II.- EXPERIMENTAL PRESSURE COEFFICIENTS FOR A 33-1/3-CALIBER OGIVE-CYLINDER MODEL AT VARIOUS ANGLES OF ATTACK. $M_o = 1.98$, $Re_o = 0.5 \times 10^6$/INCH, MODEL 2 - Concluded

(g) $\alpha = 15.1^\circ$

$\frac{x}{d}$	Radial angle, θ																		
	0°	15°	30°	45°	60°	75°	90°	105°	120°	135°	150°	165°	180°	195°	210°	225°	240°	255°	270°
0.44	0.345	0.332	0.267	0.192	0.106	0.024	-0.044	-0.074	-0.060	-0.052	-0.055	-0.041	-0.021	-0.054	-0.049	-0.052	-0.070	-0.068	-0.017
.89	.335	.323	.265	.196	.111	.027	-.047	-.087	-.072	-.064	-.063	-.060	-.011	-.054	-.060	-.064	-.088	-.088	-.056
1.33	.319	.300	.238	.167	.081	-.002	-.072	-.096	-.078	-.073	-.077	-.045	-.014	-.073	-.071	-.073	-.096	-.096	-.062
1.78	.286	.271	.211	.140	.060	-.021	-.089	-.110	-.089	-.078	-.087	-.058	-.023	-.081	-.088	-.084	-.108	-.108	-.082
2.22	.265	.249	.190	.120	.041	-.038	-.105	-.134	-.109	-.075	-.093	-.059	-.030	-.088	-.089	-.071	-.131	-.131	-.094
2.67	.240	.229	.171	.104	.027	-.051	-.118	-.158	-.129	-.075	-.083	-.072	-.039	-.085	-.086	-.077	-.157	-.155	-.113
3.11	.228	.211	.153	.085	.009	-.066	-.133	-.177	-.129	-.073	-.063	-.066	-.045	-.066	-.067	-.032	-.174	-.172	-.122
3.56	.200	.190	.132	.069	-.004	-.077	-.144	-.191	-.147	-.077	-.066	-.065	-.052	-.060	-.067	-.033	-.190	-.188	-.138
4.00	.176	.154	.111	.050	-.021	-.092	-.158	-.208	-.148	-.080	-.071	-.068	-.059	-.062	-.071	-.034	-.208	-.205	-.154
4.44	.151	.131	.090	.031	-.038	-.108	-.171	-.219	-.144	-.091	-.079	-.074	-.063	-.068	-.078	-.095	-.223	-.220	-.170
4.89	.133	.114	.074	.018	-.049	-.118	-.182	-.216	-.136	-.104	-.084	-.075	-.061	-.071	-.083	-.110	-.222	-.222	-.181
5.33	.115	.096	.057	0	-.066	-.132	-.193	-.204	-.132	-.119	-.096	-.084	-.063	-.076	-.093	-.128	-.208	-.210	-.195
5.78	.102	.084	.046	-.010	-.074	-.138	-.200	-.189	-.129	-.125	-.110	-.092	-.060	-.082	-.105	-.131	-.187	-.188	-.204
6.22	.092	.075	.042	-.015	-.083	-.152	-.212	-.169	-.127	-.138	-.126	-.105	-.051	-.087	-.122	-.133	-.166	-.172	-.207
6.67	.096	.074	.032	-.016	-.093	-.158	-.206	-.151	-.123	-.134	-.144	-.123	-.039	-.096	-.139	-.132	-.134	-.137	-.201
7.11	.086	.068	.029	-.027	-.093	-.159	-.186	-.116	-.108	-.109	-.147	-.134	-.041	-.107	-.150	-.116	-.115	-.118	-.183
7.55	.086	.068	.026	-.033	-.099	-.163	-.168	-.100	-.097	-.107	-.152	-.130	-.034	-.103	-.150	-.095	-.092	-.093	-.162
8.00	.084	.061	.020	-.037	-.102	-.168	-.155	-.092	-.089	-.110	-.153	-.136	-.033	-.099	-.132	-.097	-.077	-.078	-.154
8.44	.086	.065	.023	-.037	-.107	-.169	-.137	-.084	-.086	-.111	-.138	-.131	-.036	-.101	-.130	-.103	-.071	-.073	-.119
8.89	.081	.061	.019	-.040	-.108	-.167	-.109	-.077	-.082	-.107	-.132	-.117	-.049	-.105	-.123	-.094	-.071	-.071	-.087
9.33	.092	.068	.024	-.038	-.108	-.163	-.086	-.066	-.070	-.095	-.114	-.110	-.046	-.094	-.098	-.080	-.063	-.063	-.075
9.78	.082	.059	.018	-.041	-.110	-.159	-.076	-.067	-.070	-.086	-.094	-.111	-.056	-.086	-.077	-.072	-.064	-.064	-.071
10.22	.088	.064	.020	-.041	-.110	-.156	-.072	-.066	-.068	-.075	-.076	-.090	-.050	-.074	-.059	-.060	-.067	-.068	-.076
10.67	.082	.061	.018	-.043	-.113	-.156	-.085	-.072	-.072	-.069	-.070	-.086	-.046	-.062	-.052	-.057	-.068	-.068	-.087
11.33	.072	.054	.012	-.048	-.116	-.152	-.110	-.071	-.066	-.062	-.062	-.073	-.046	-.052	-.048	-.054	-.064	-.065	-.116
12.00	.078	.054	.010	-.051	-.119	-.142	-.136	-.065	-.058	-.057	-.062	-.062	-.038	-.041	-.042	-.046	-.060	-.062	-.135
12.67	.081	.049	.005	-.055	-.100	-.158	-.143	-.058	-.051	-.050	-.057	-.061	-.038	-.037	-.039	-.043	-.061	-.064	-.157
13.33	.080	.053	.012	-.038	-.100	-.162	-.146	-.055	-.048	-.043	-.048	-.058	-.041	-.037	-.038	-.042	-.059	-.062	-.164
14.00	.091	.065	.023	-.037	-.106	-.164	-.131	-.051	-.045	-.041	-.045	-.048	-.033	-.030	-.036	-.040	-.068	-.069	-.164

NACA

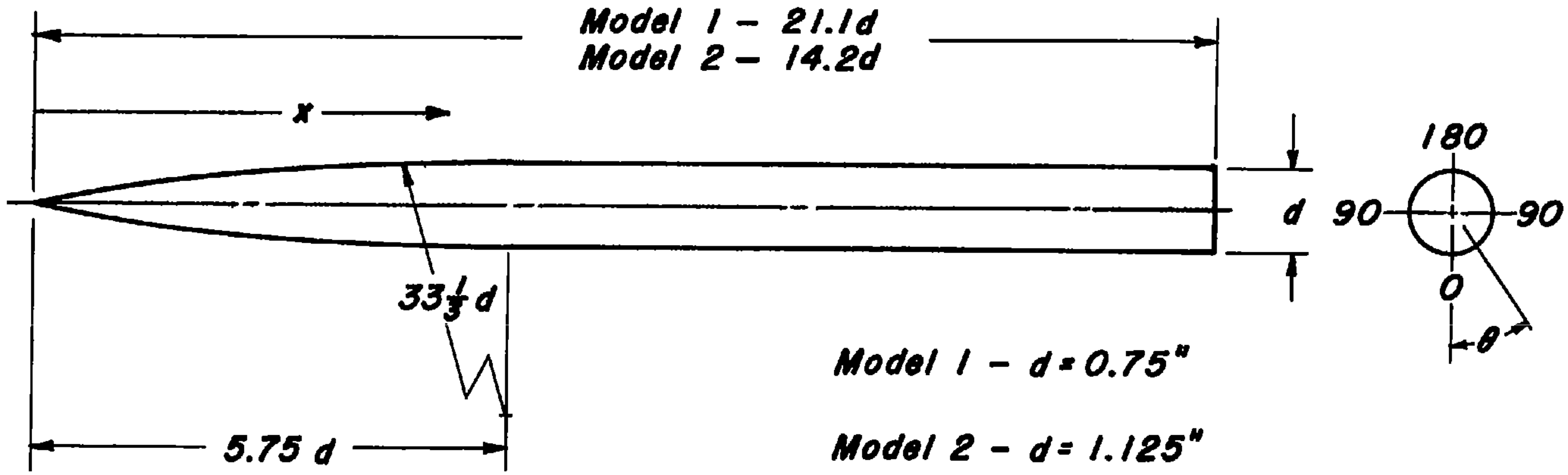

Orifice size: 0.030" dia.

Orifice location: Model 1 - longitudinal rows at $\theta = 0°, 90°, 180°$
longitudinal spacing 0.667d for $6.08 < x/d < 20.75$

Model 2 - longitudinal row at $\theta = 0°$
longitudinal spacing 0.444d for $0.44 < x/d < 10.67$
0.667d for $10.67 < x/d < 14.00$

Figure 1.– Model dimensions and orifice locations.

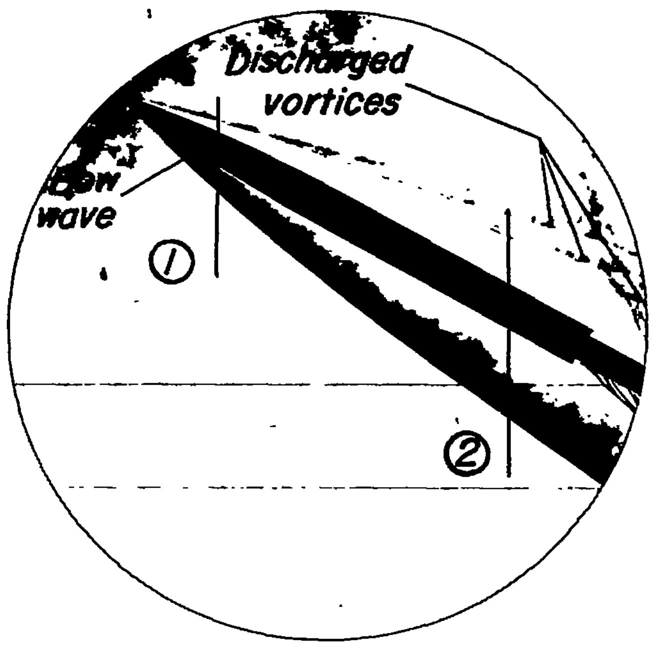

(a) Side view schlieren photograph.

(b) Vapor-screen photograph forward station.

(c) Vapor-screen photograph rearward station.

Figure 2.- Schlieren and vapor-screen photographs showing vortex configuration for an inclined body of revolution. $\alpha \cong 30^{\circ}$, $M_0 \cong 2.0$.

NACA
A-17693

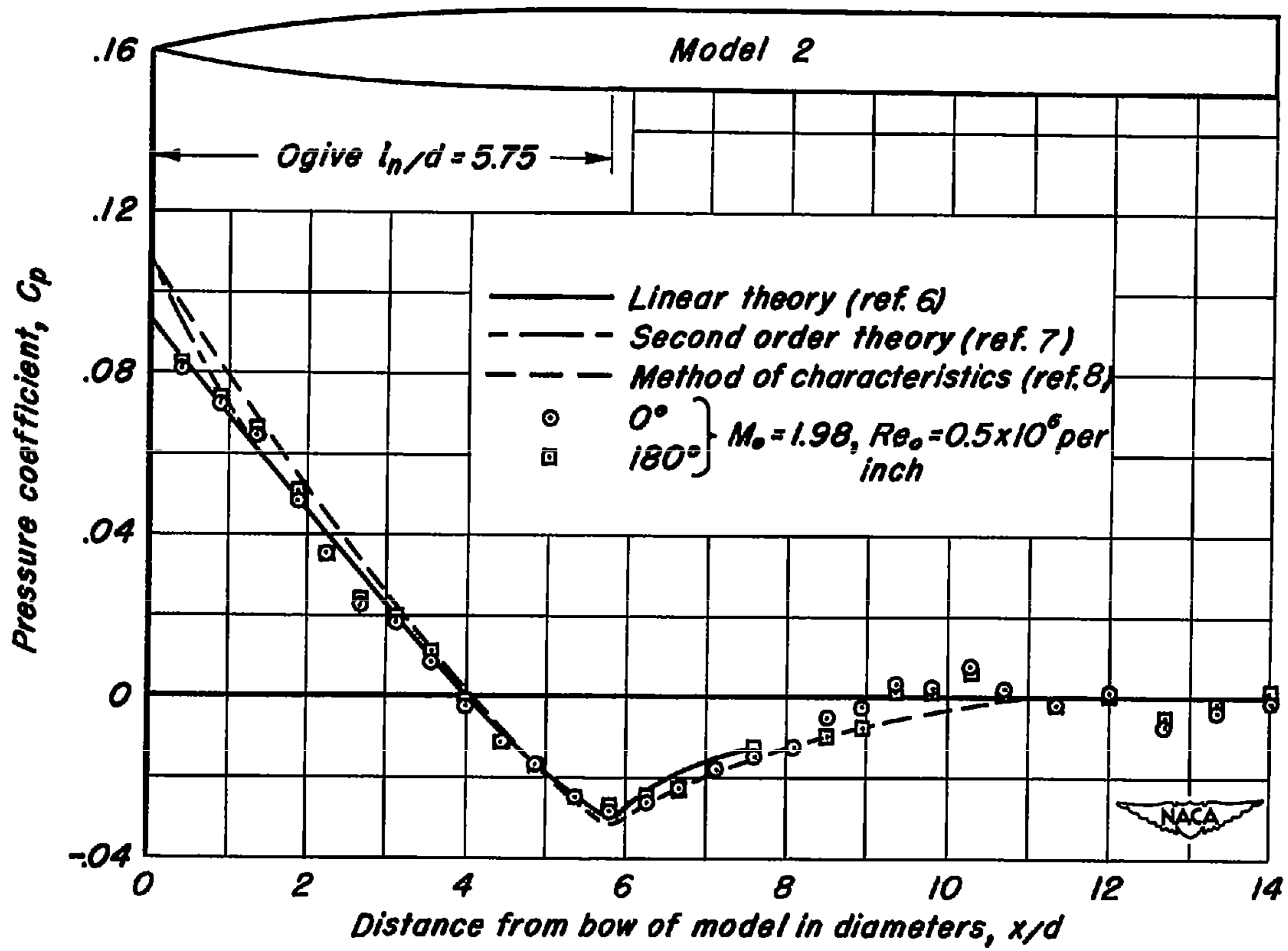

Figure 3.– Comparison of theoretical and experimental longitudinal pressure distribution at zero angle of attack.

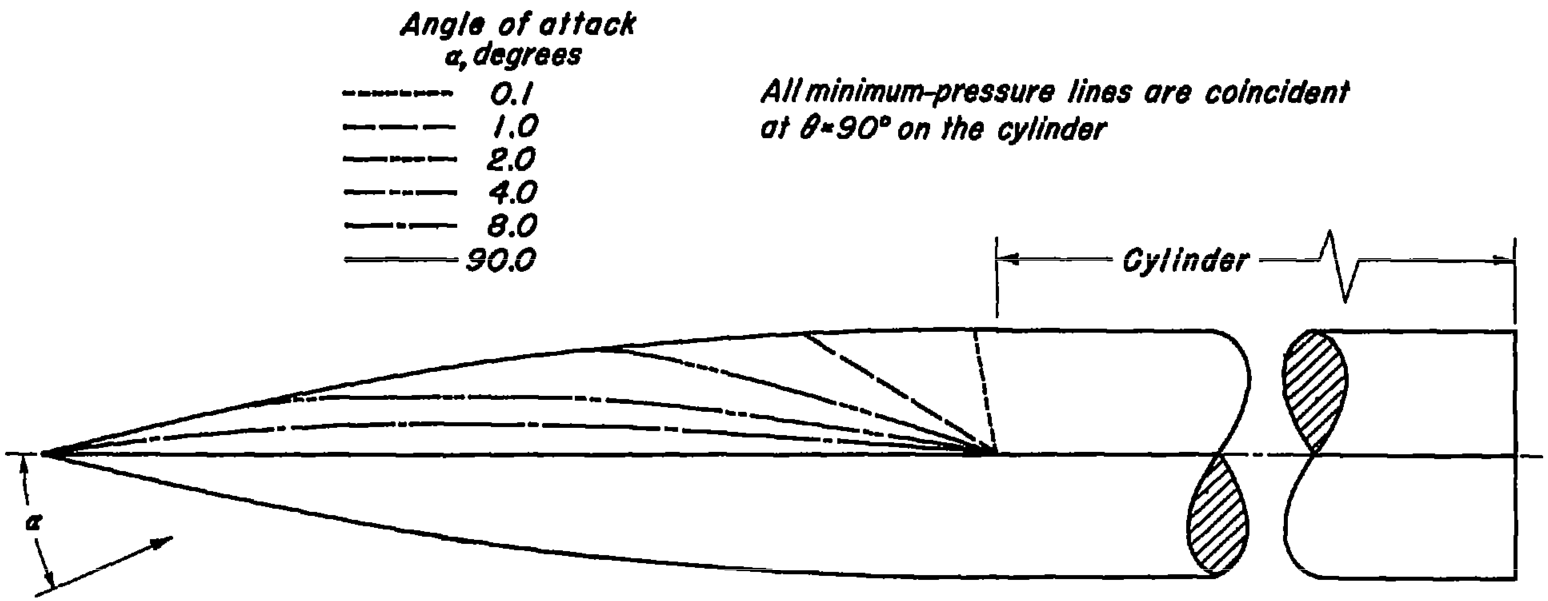

Figure 4.— Theoretical minimum-pressure lines for the cross-flow about the model for various angles of attack.

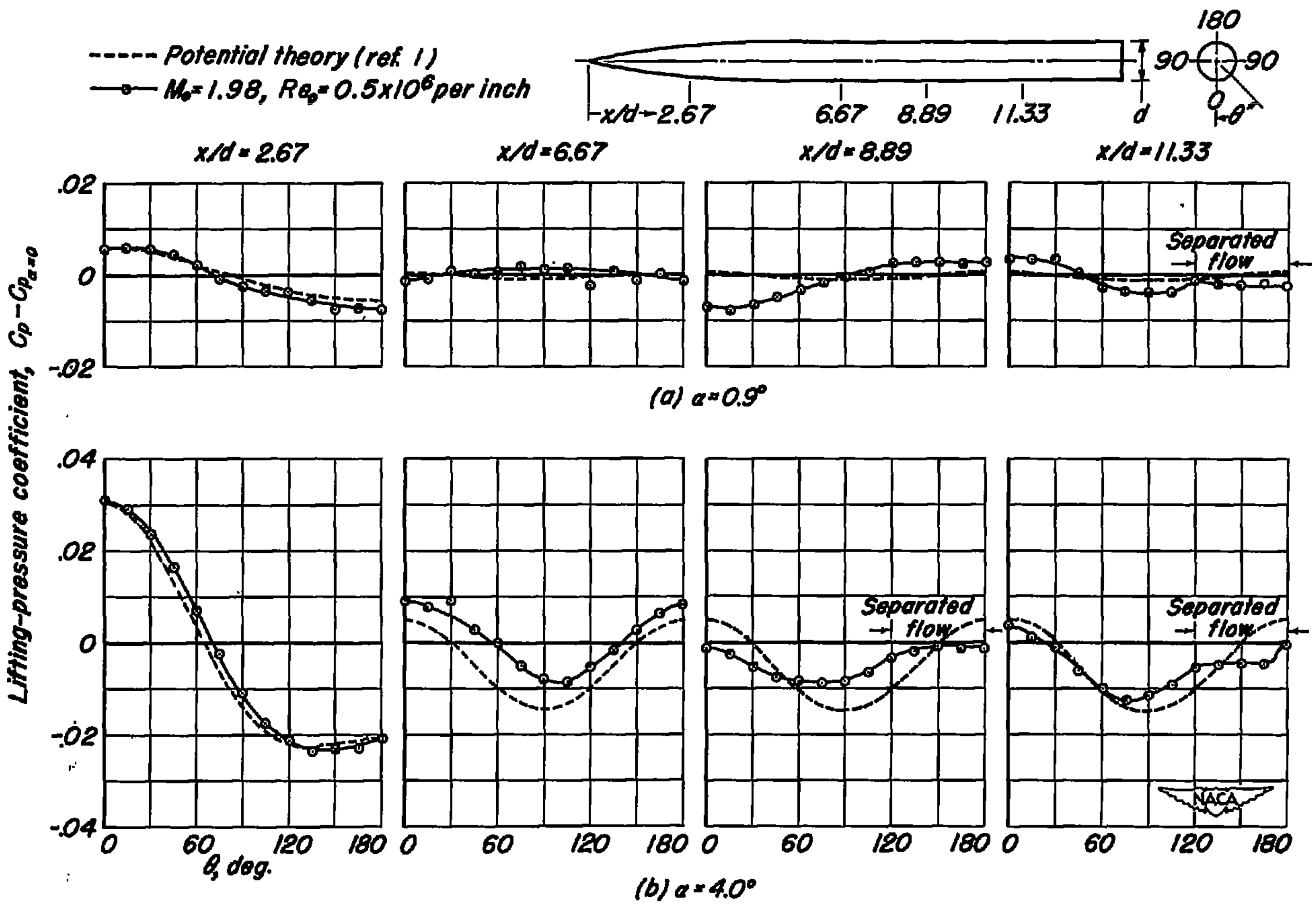

Figure 5.– Comparison of theoretical and experimental circumferential distribution of lifting pressure. ($0 \leq \alpha \leq 15.1°$)

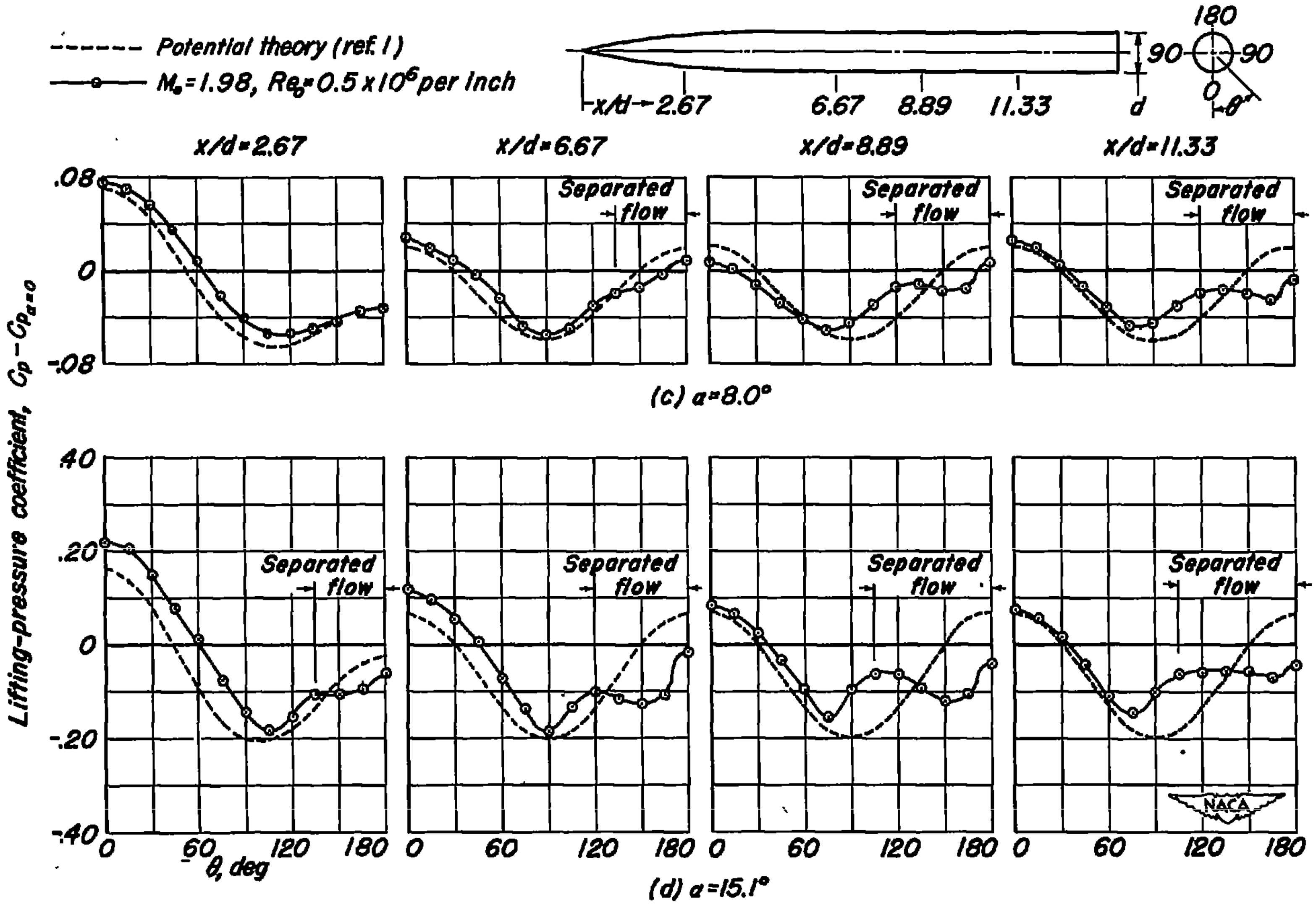

Figure 5.— Concluded.

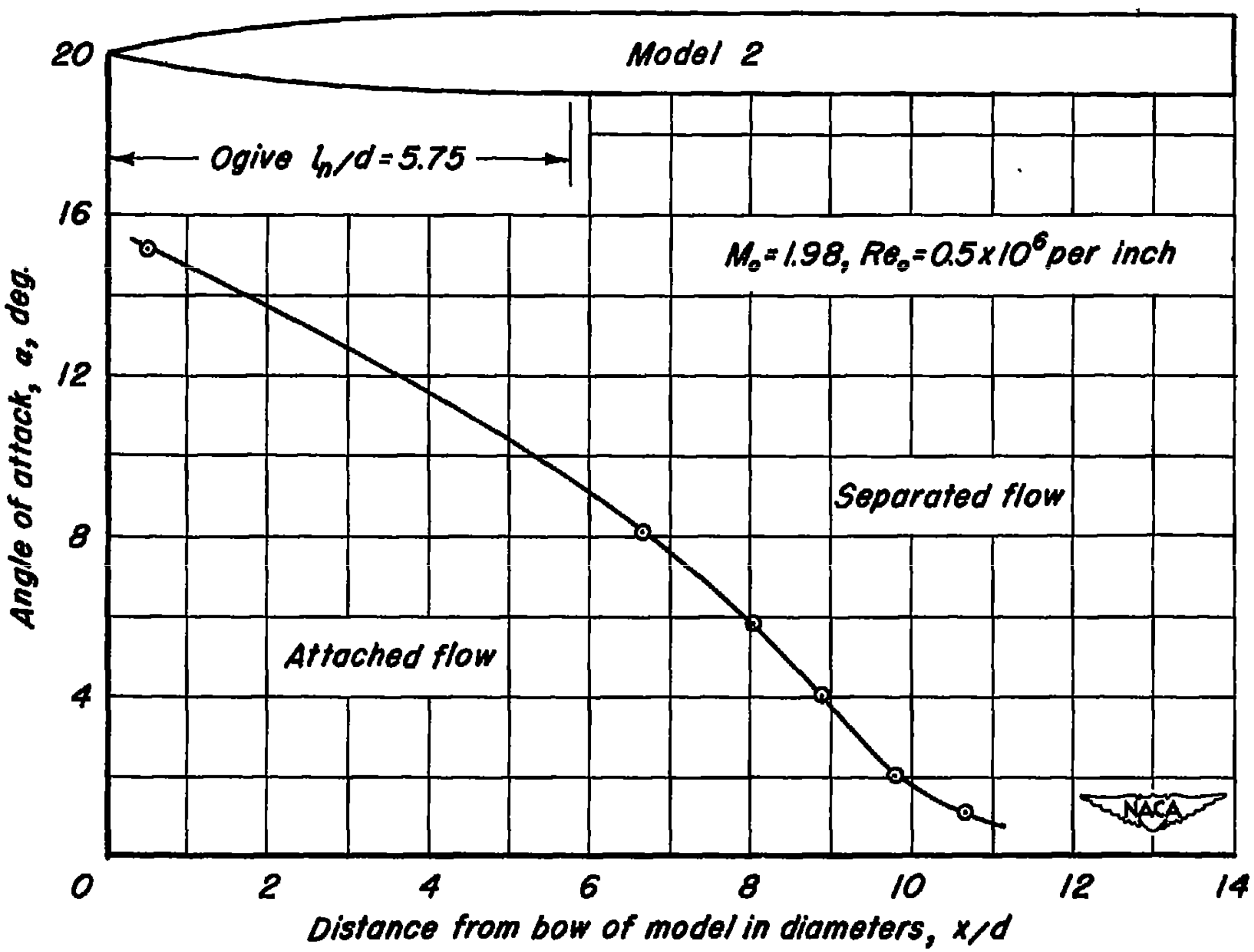

Figure 6.- Longitudinal position at which cross-flow separation first occurs at various angles of attack.

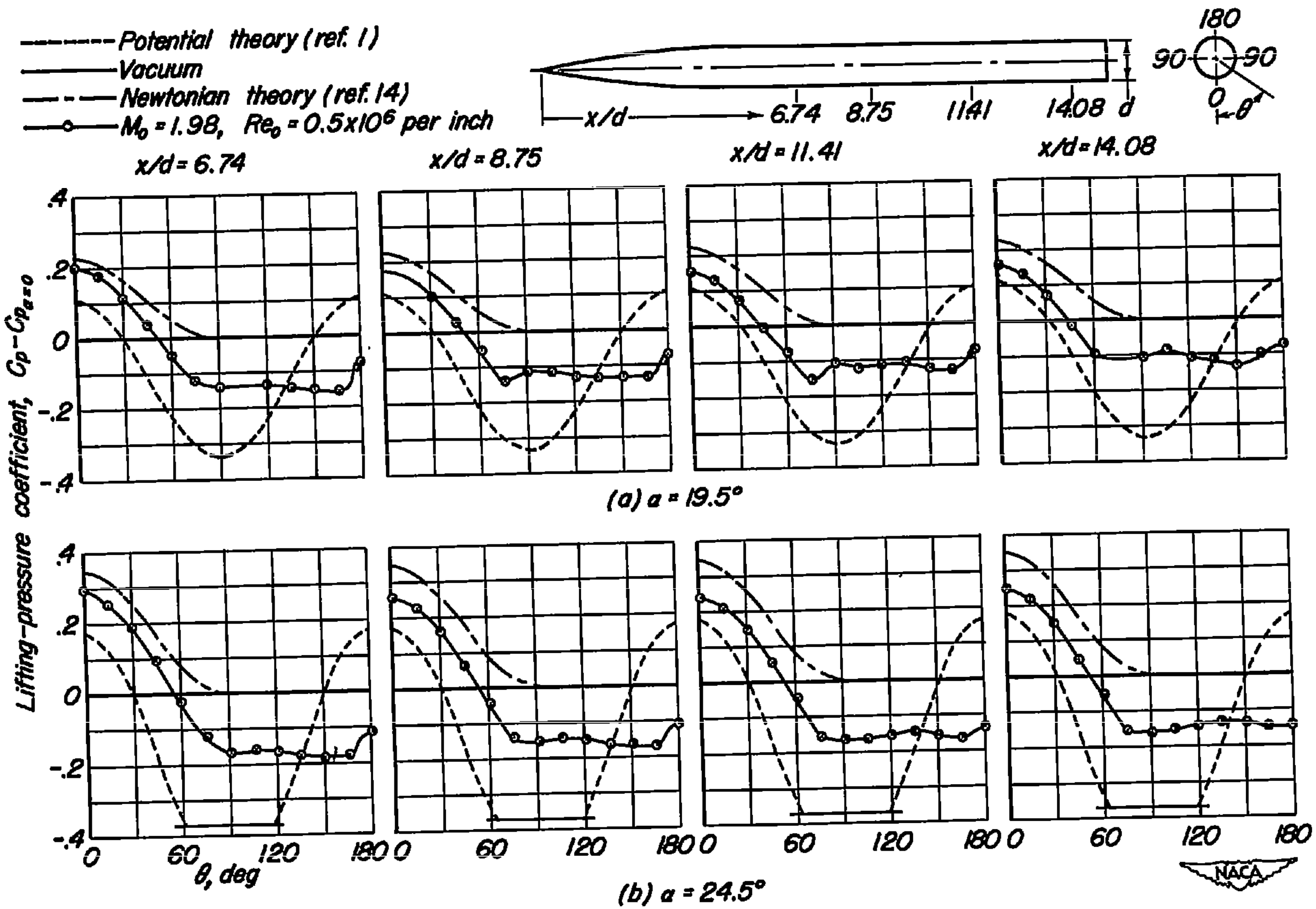

Figure 7.– Comparison of theoretical and experimental distribution of lifting pressure ($19.5° \leq \alpha \leq 35.5°$).

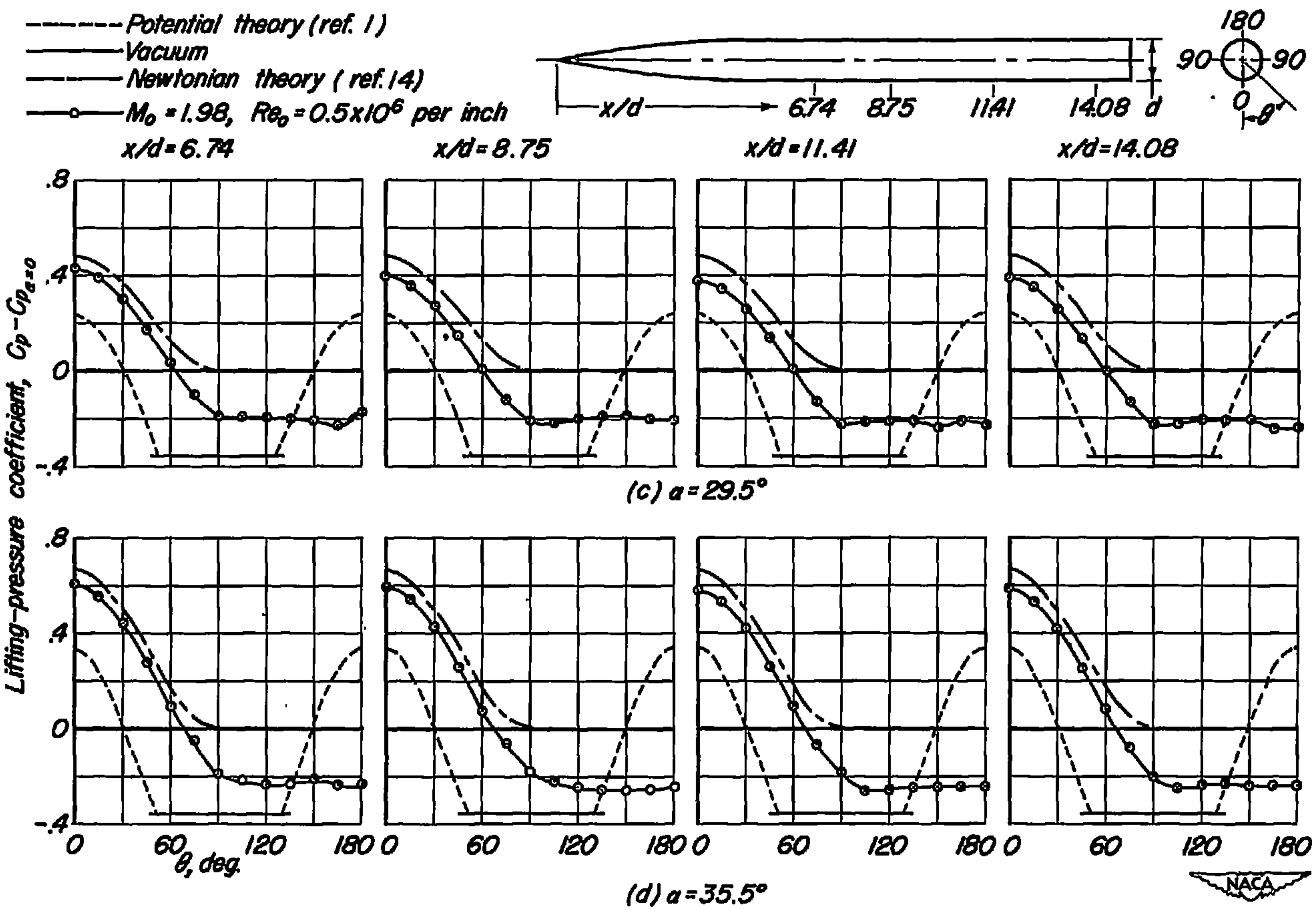

Figure 7. — Concluded.

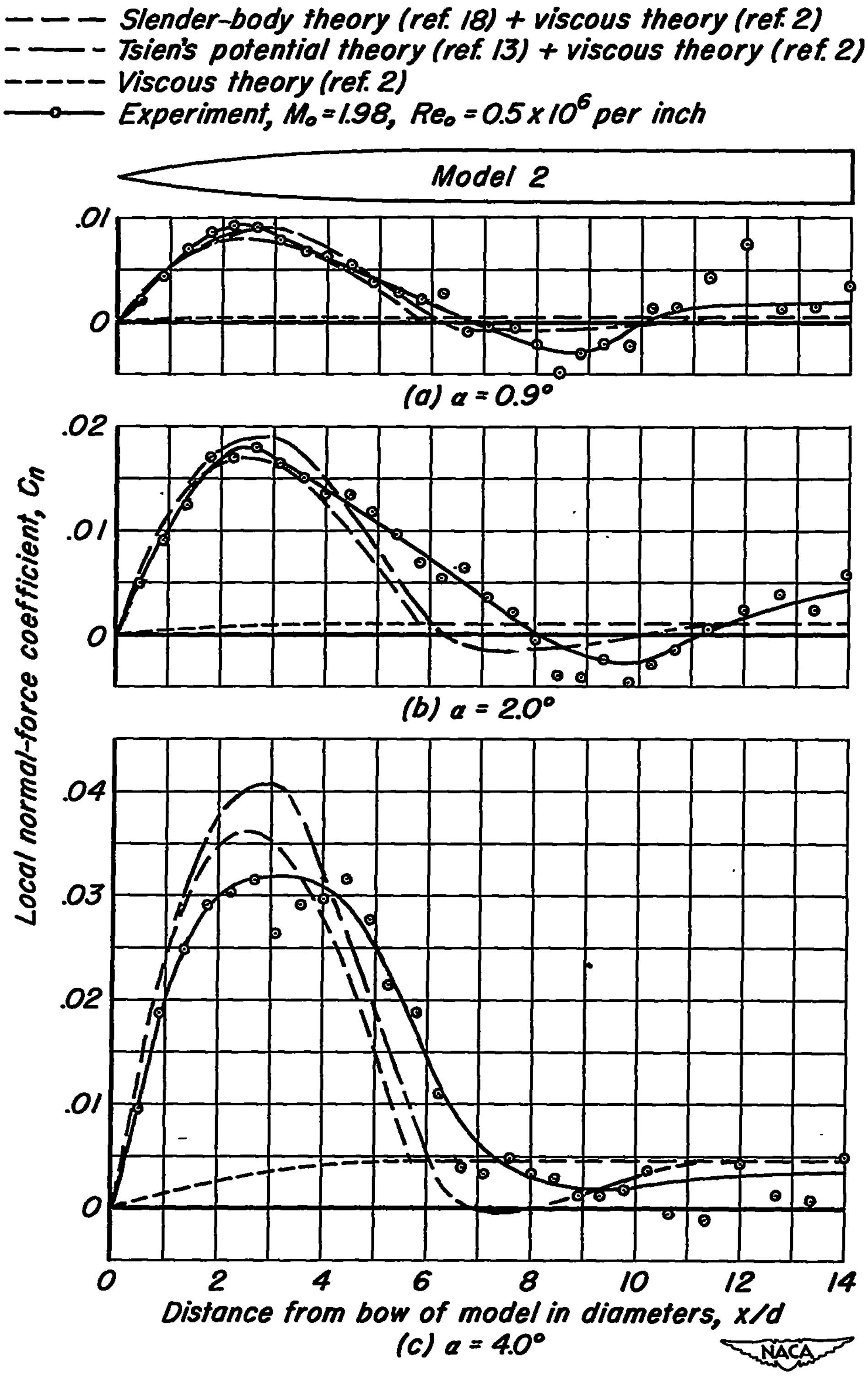

Figure 8.– Comparison of theoretical and experimental normal-force distribution at various angles of attack.

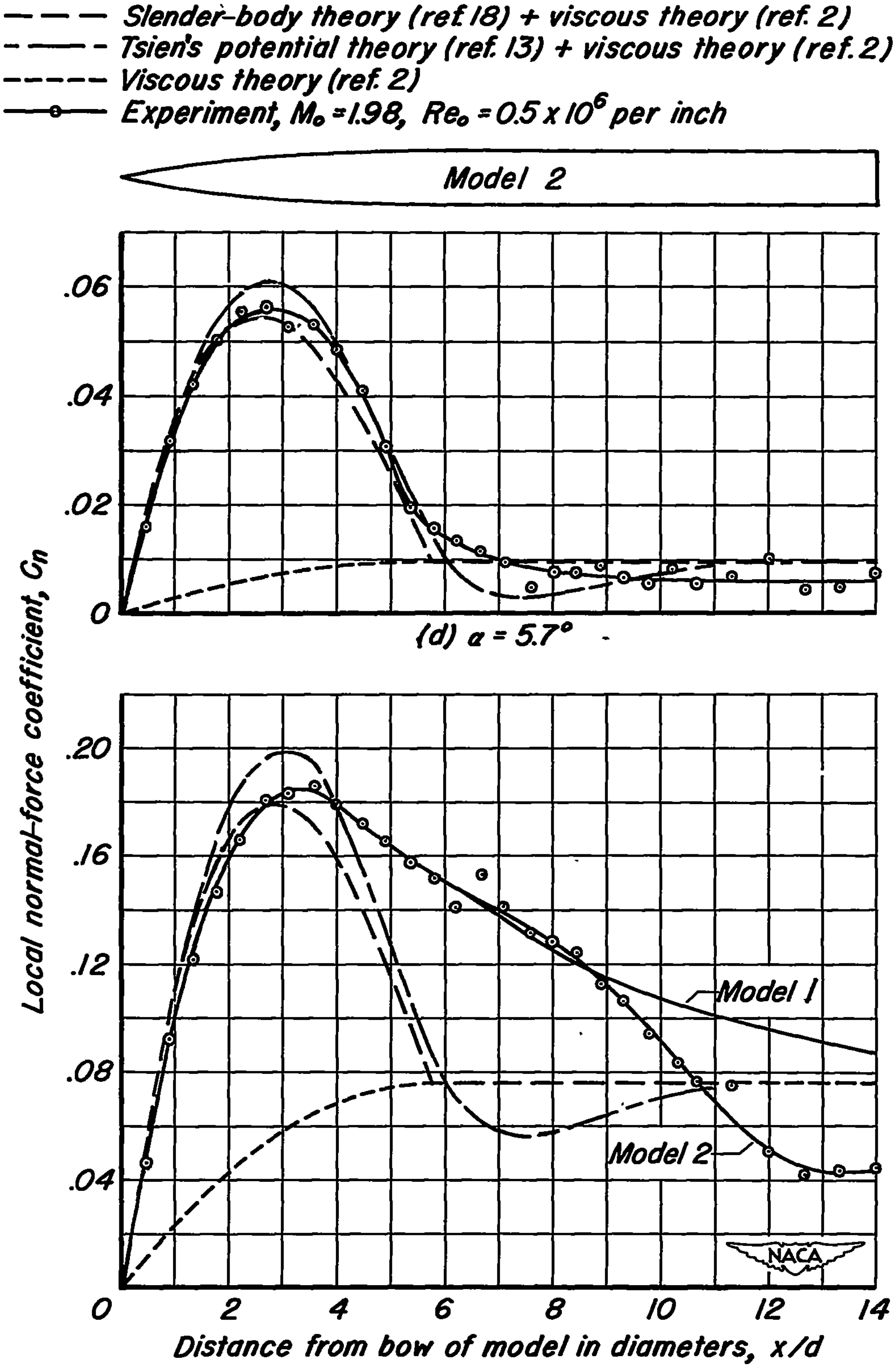

(e) α = 15.1°

Figure 8.—Concluded.

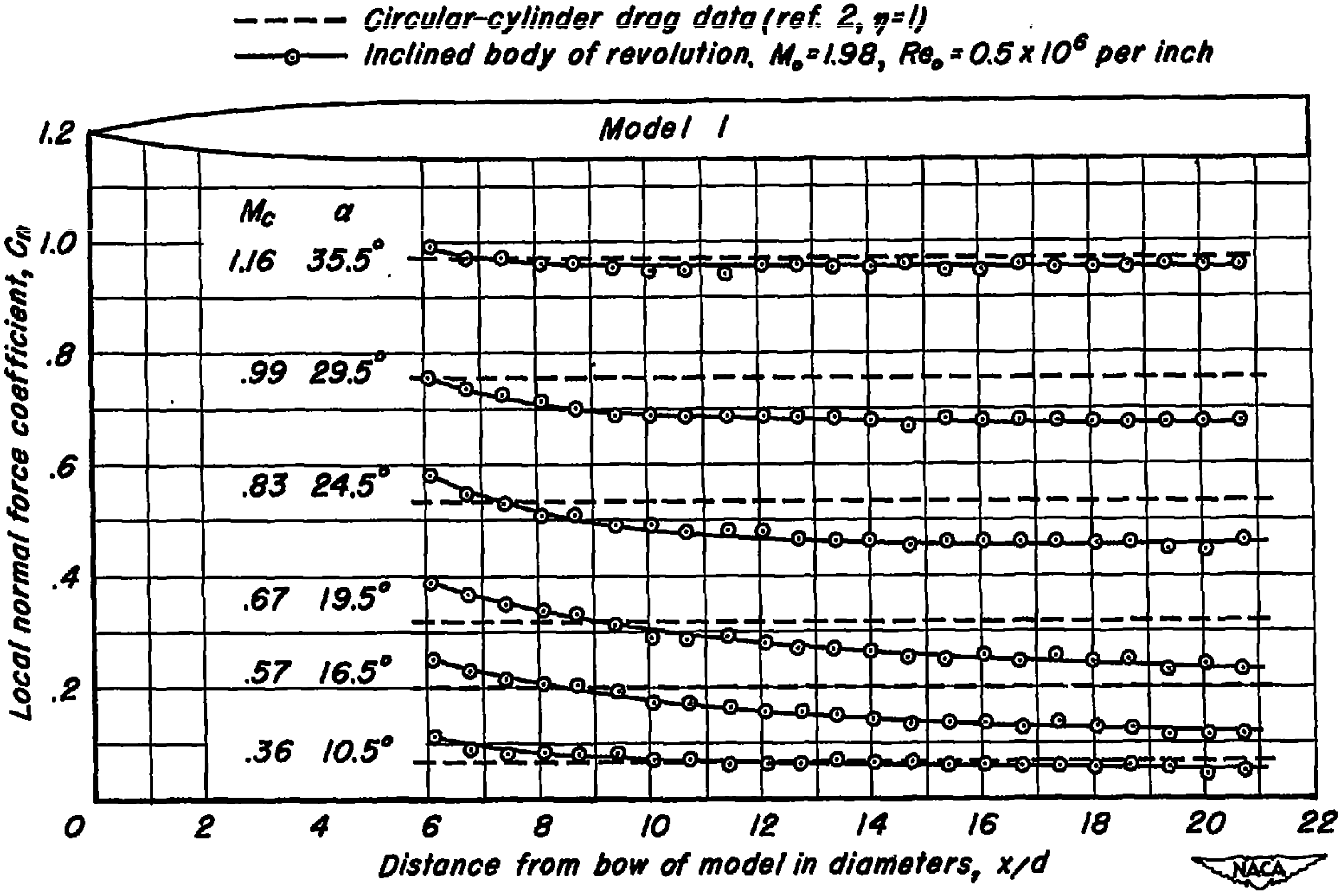

Figure 9.- Comparison of circular-cylinder drag data and experimental normal-force distribution at various angles of attack.

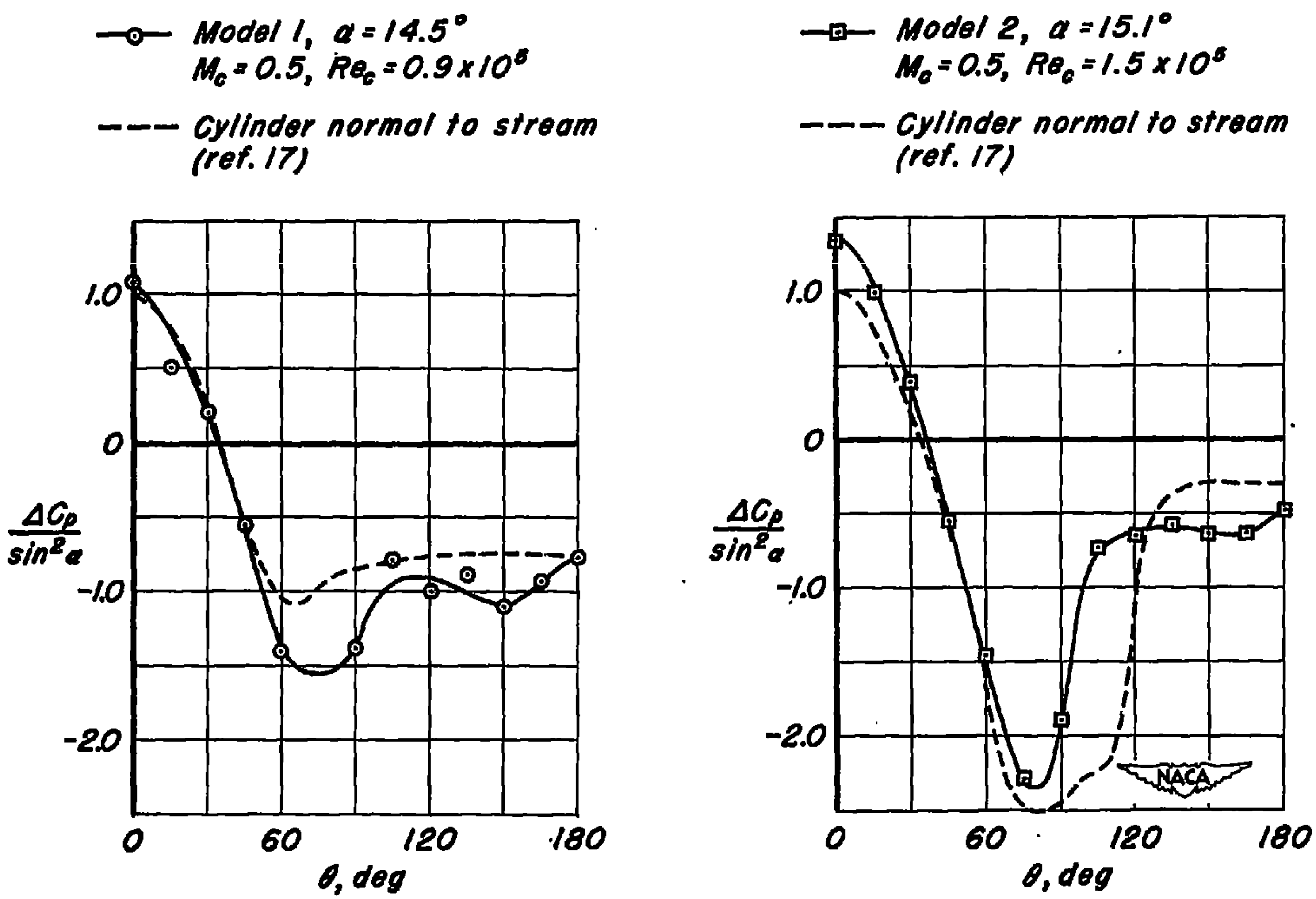

Figure 10.- Cross-flow Reynolds number effect on the circumferential pressure distribution $x = 14d$.

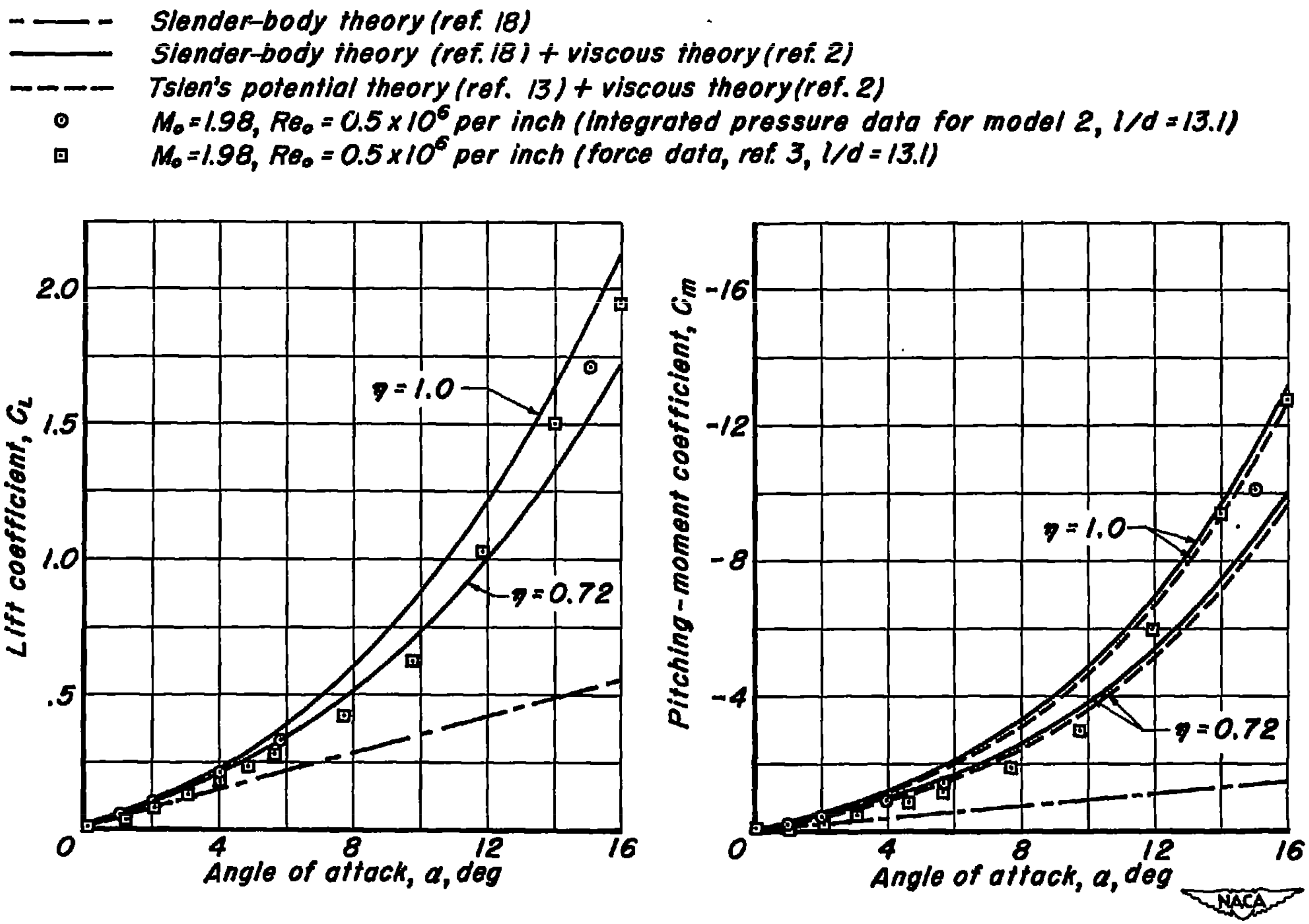

Figure 11.- Comparison of theoretical and experimental lift and pitching-moment characteristics.

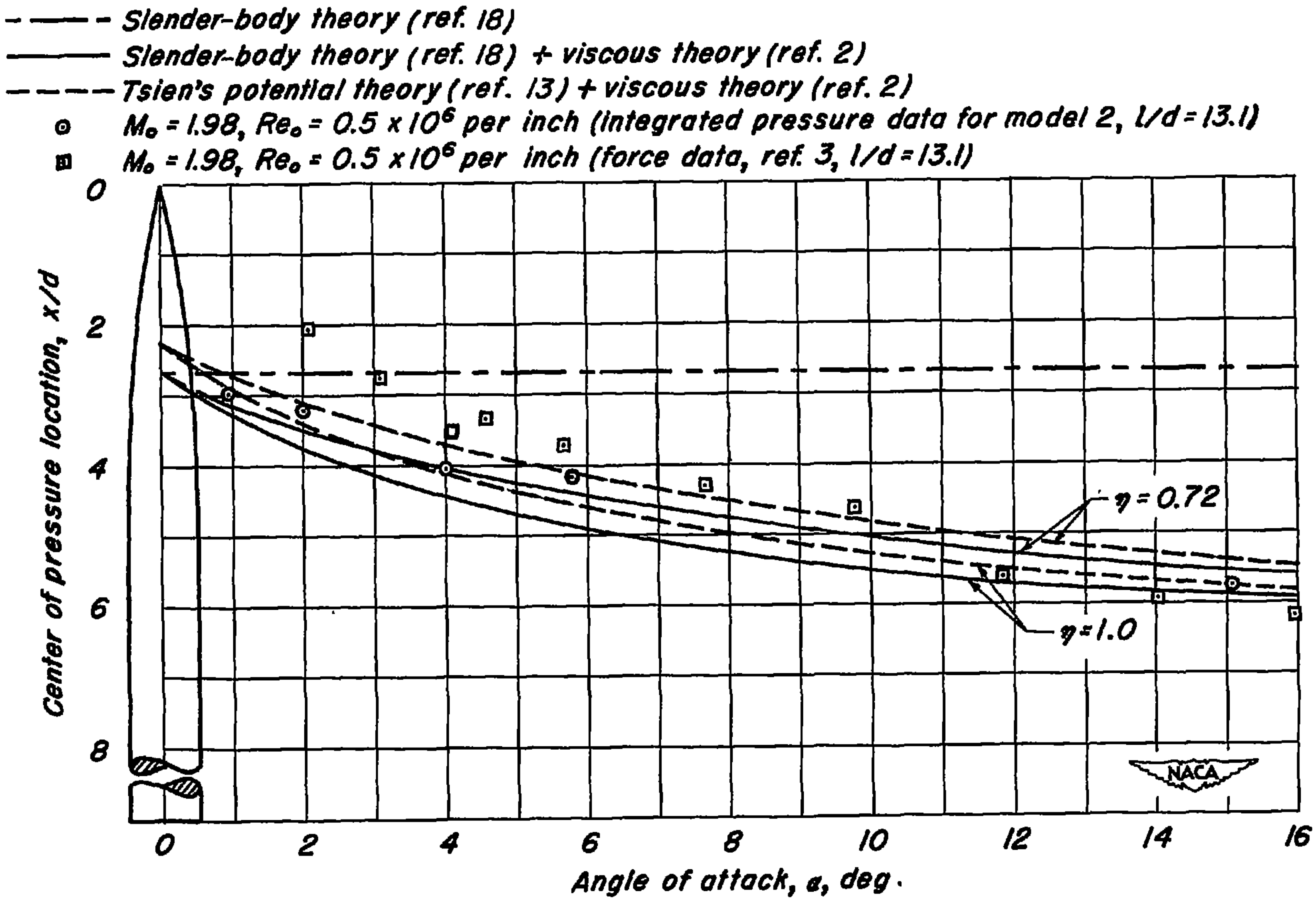

Figure 12.- Comparison of theoretical and experimental center-of-pressure location.